CHAPTER 4

PREPARATION, OPTIMIZATION AND CHARACTERIZATION OF CONJUGATED NANOPARTICLES

4 PREPARATION, OPTIMIZATION AND CHARACTERIZATION OF CONJUGATED NANOPARTICLES

4.1 Introduction

There are varieties of nanoconstructs systems currently being explored for therapeutic delivery. There is an increased interest in developing biodegradable Nanoparticles (NPs) since they offer a suitable means of delivering small molecular weight drug, protein or gene by either localized or targeted delivery to the tissue of interest (Moghimi SM et al., 2001). The types of Nanoparticles (NPs) currently used in research for therapeutic applications include dendrimers, liposomes, polymeric NPs, micelles, protein NPs, ceramic NPs, viral NPs, metallic NPs, and carbon nanotubes. (Byrne JD et al., 2008). Amongst these nanoparticulate delivery systems polymeric NPs have shown promising properties for targeted drug delivery and for sustained action. NPs are colloidal systems that range in size typically from 10 to 1000 nm in diameter, and are formulated from a biodegradable polymer in which the therapeutic agent is entrapped in, adsorbed or chemically coupled onto the polymer matrix (Labhasetwar V, 1997). Biodegradable polymers are unique tools for the preparation of NPs, owing to their low toxicity profiles. (Feng SS, 2004) Despite the potential promise of cyanoacrylate polymers for brain targeting, the clinical safety of cyanoacrylates has not yet been established. Although a number of different polymers have been investigated for formulating biodegradable NPs, polyepsilon caprolactone (PCL), poly (lactide-co-glycolide) (PLGA) and poly lactic acid (PLA), FDA approved biocompatible and biodegradable polymers, have been the most extensively studied (Langer R, 1997; Jain RA, 2000).

NPs can be prepared by polymerization of monomers entrapping the drug molecules leading to insitu polymerization or from preformed polymers. Several techniques have been suggested to prepare the biodegradable polymeric NPs from preformed polymers such as poly (D, L-lactide) {PLA}, poly (D, L-glycolide) {PGA} and poly (D,L-lactide-co-glycolide) {PLGA}. Various methods proposed for the preparation of PLGA NPs include emulsification/solvent evaporation, solvent displacement/diffusion (nanoprecipitation), emulsification/solvent diffusion and salting out using synthetic polymers. Solvent diffusion (nanoprecipitation method) leads to the NPs of uniform size and narrow size distribution. (Fessi H et al., 1989) The Nanoprecipitation method involves a spontaneous gradient driven diffusion of amphiphilic organic solvent into continuous phase. The energy released in this process leads to rapid dispersion of polymer rich organic phase in the form of nanodroplets.

Following the initial precipitation of the polymer forming the nanospheres matrix, final solidification of the resultant nanospheres matrix is accomplished by evaporating the organic solvents (Michael C et al., 2002). Polyvinyl alcohol (PVA) is used as stabilizer to form particles of relatively small size and uniform size distribution (Sahoo SK et al., 2002; Scholes PD et al., 1993).

Various formulation and process variables relating to effectiveness, safety, and usefulness should be optimized simultaneously when developing pharmaceutical formulations. The difficulties in optimizing a pharmaceutical formulation are due to the difficulty in understanding the real relationship between casual and individual pharmaceutical responses. A factorial design has often been applied to optimize the formulation variables (Misra A and Sheth AK, 2002; Levison KK et al., 1994; Shirakura O et al., 1991). The optimization procedure based on Response surface methodology (RSM) includes statistical experimental designs, multiple regression analysis, and mathematical optimization algorithms for seeking the best formulation under a set of constrained equations. Since theoretical relationships between the response variables and causal factors are not clear, multiple regression analysis can be applied to the prediction of response variables on the basis of a second-order equation. In the present study, drug: polymer ratio, %w/v PVA concentration and volume of organic phase were selected as independent variables, whereas particle size (PS) and % entrapment efficiency (EE) were selected as dependent variables.

Surface modification of PLGA NPs has been attempted by either conjugating their surface with different ligands or conjugating ligands to the polymer followed by preparation of NPs. Ligands which have been reported are folic acid (Stella B et al., 2000), transferring (Tf) (Sahoo SK et al., 2004), lactoferrin (Lf) (Huang RQ et al., 2010) biotin (Minko T, 2004), lectins (Sharma A et al., 2004) etc These ligands bind specifically to the receptors on the plasma membrane of the target tissue which leads to the internalization of plasma membrane receptors along with the delivery system i.e. NPs.

PVA cross links with PLGA during the NPs formation. The hydroxyl groups of PVA at the surface of NPs are useful for the conjugation of ligand to the NPs surface. The NPs are first activated by reaction of epoxy group of polyglycidyl glycerol ether with the hydroxyl of PVA in the presence of zinc tetrafluoro borohydrate as catalyst. The activated NPs are then reacted with ligand by linkage of the amino group of ligand with another epoxy of the polyglycidyl glycerol ether. The reaction of epoxy group is favoured at pH 5.0 (Sahoo SK et al., 2004).

4.2 Methods

4.2.1 Preparation and Optimization of Nanoparticles

The nanoprecipitation technique involves the use of water miscible organic solvents to solubilize both the drug and polymer. Addition of organic phase leads to rapid diffusion of the solvent toward the aqueous phase which results in intensive spreading of the organic polymer solution and formation of emulsion droplets of submicron size followed by polymer precipitation in the form of nanodispersion. The NPs of both the drugs Tramadol (TMD) and Lamotrigine (LTG) were prepared using the solvent diffusion (nanoprecipitation) technique (Fessi H et al., 1989).

4.2.1.1 Preliminary Optimization of various Formulation Parameters

Selection of organic phase is critical for nanoprecipitation method affecting product attributes. Also, the basic process parameters like rate of addition of organic phase and the speed of the magnetic stirrer were standardized before proceeding for the optimization of the formulation parameters.

4.2.1.1.1 Selection of Organic Phase

Water miscibility of the organic solvents play critical role in the formation of NPs. through nanaoprecipitation technique, as it will affect the diffusion rate thereby final mean size and drug entrapment. Solvent dielectric constant is related to the miscibility, the more the dielectric constant of the solvent, the more it is water miscible, leading to the production of small particles (Bilati U et al., 2005). Different water miscible organic solvents namely acetone, acetonitrile and tetrahydrofuran (THF) were used for the preparation of NPs. The polarity index, evaporation rate [compared to butyl acetate (BuAc)] and boiling point range of acetone, acetonitrile and THF are given in the Table 4.1.

Table 4.1: Polarity index, evaporation rate and boiling point range of solvents

Solvent	Polarity index	Evaporation rate (BuAc)	Boilingrange (°C)
Acetonitrile	5.8	5.79	81-83
Acetone	5.1	7.7	53-55
Tetrahydrofuran	4.0	8.0	63-66

4.2.1.1.2 Optimization of process parameters

As known from the literature, the rate of addition of organic phase was kept at 0.5 ml/min throughout the entire optimization process. The speed of the stirrer for further experiments was standardized using qualitative examination of NPs dispersion. The process parameters were standardized using placebo batches without drug.

4.2.1.2 Factorial design and optimization of formulation parameters

4.2.1.2.1 Preparation of NPs

Drug loaded PLGA NPs were prepared by nanoprecipitation technique shown in Fig. 4.1, as described by Fessi H et al., 1989. On the basis of the preliminary experimentation critical formulation parameters were viz. drug: polymer ratio, % PVA concentration and organic: aqueous phase ratio. Briefly, 10 mg TMD and PLGA (50, 75 and 100 mg corresponding to 1: 5, 1: 7.5 and 1: 10 drug: polymer ratio) were accurately weighed and dissolved in the acetone (2.5, 3.3 and 5 ml corresponding to organic: aqueous phase volume ratio of 1:4, 1:3 and 1:2). The organic phase was added drop wise using syringe (BD Discardit II^{TM} syringe with 26G ½, 0.45mm X 13 mm needle) into 10 ml of aqueous phase containing PVA (0.5, 1 and 1.5% w/v) as stabilizer under gentle magnetic stirring (Remi Equipments, Mumbai). TMD loaded NPs formed immediately with the spontaneous diffusion of solvent in to the aqueous phase. With the diffusion of solvent in to the aqueous phase, the polymer precipitates while encapsulation of TMD also occur leading to formation TMD-NPs. The resulting NPs dispersion was further stirred to evaporate the organic phase. NPs were recovered by centrifugation at 20,000 rpm for 30 min and washed twice with distilled water to remove excess PVA.

LTG loaded NPs [LTG-NPs] were prepared using the same procedure with lower amount of PLGA (40, 60 and 80 mg corresponding to 1: 5, 1: 7.5 and 1: 10 drug: polymer ratio)

Figure 4.1: Schematic representation of the nanoprecipitation process

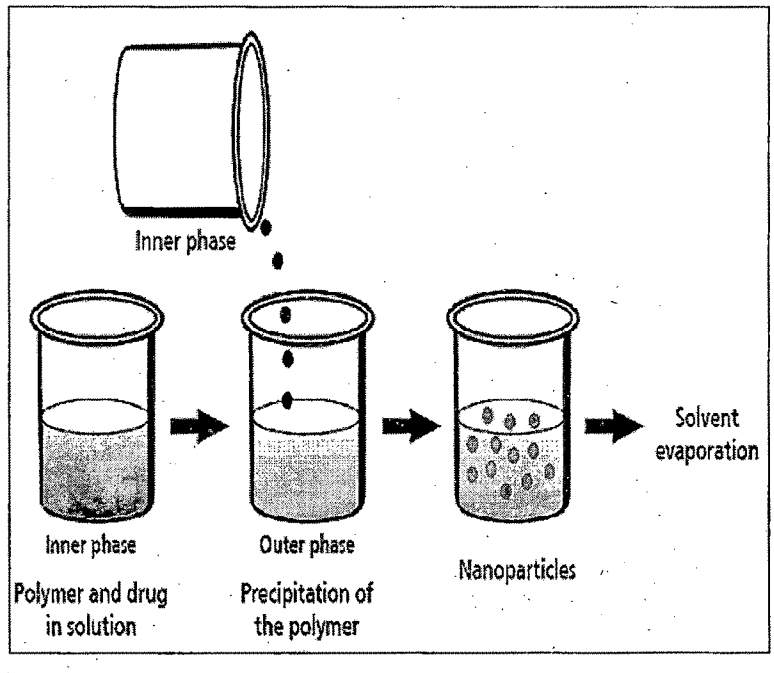

4.2.1.2.2 Optimization of formulation parameters

Pharmaceutical formulations are effected by single or combination of variables. It is difficult to assess the effect of the variables individually or in combination. Factorial designs allow all the factors to be varied simultaneously, thus enabling evaluation of the effects of each variable at each level and showing interrelationship among them. Factorial designs are of choice when simultaneous determination of the effects of several factors and their interactions on response parameters is required. A prior knowledge and understanding of the process and the process variables under investigation are necessary for achieving a more realistic model. Initial experiments revealed the critical role of polymer concentration, stabilizer concentration and organic: aqueous phase ratio as major variables in determining the PS and drug entrapment efficiency. Hence, polymer concentration, % w/v PVA concentration and organic: aqueous phase ratio were selected as independent variables to find the optimized condition for small PS (PS) (<150 nm) and higher % entrapment efficiency (% EE) using 3^3 factorial design and contour plots, whereas PS and % EE were selected as response variables. The values of these selected variables along with their transformed values are shown in Table 4.3.

Table 4.2: Coded values of the formulation parameters for TMD-NPs and LTG-NPs

Coded values	Actual values		
	Stabilizer concentration X_1 (% w/v)	Polymer Concentration X_2 (mg)	Volume of organic phase X_3 (ml)
-1	0.5	50/40*	2.5
0	1	75/60*	3.3
1	1.5	100/80*	5

*for preparation of LTG-NPs

Twenty seven batches of TMD and LTG NPs were prepared by nanoprecipitation method according to the 3^3 experimental design. The prepared batches were evaluated for PS, drug entrapment efficiency and the results were recorded in Table 4.4 and Table 4.5 for TMD-NPs and LTG-NPs respectively.

Multiple Regression Analysis

A multilinear stepwise regression analysis was performed using Microsoft Excel software. Mathematical modeling was carried out by using Equation 1 to obtain a second-order polynomial equation (Huang YB et al., 2005).

$$Y = b_0 + b_1X_1 + b_2X_2 + b_3X_3\, b_{11}X_1^2 + b_{22}X_2^2 + b_{33}X3^2 + b_{12}X_1X_2 + b_13X_1X_3 + b_{23}X_2X_3 + b_{123}X_1X_2X_3 \quad (1)$$

Where b_0 is the arithmetic mean response of 27 runs and b_1, b_2 and b_3 is the estimated coefficients for the factors X_1, X_2 and X_3, respectively. The major responses represent the average result obtained by changing one factor at a time from its low to high value. The interactions show the change in PS when two or more factors are varied simultaneously. Equations were was derived by the best-fit method (Akhnazarova S and Kafarov V, 1982) to describe the relationship of the PS (Y_{PS}) and entrapment efficiency (Y_{EE}) with the polymer concentration (X_1), PVA concentration (X_2) and the ratio of org. phase: aq. phase (X_3). Analysis of variance (ANOVA) of full model and reduced model (if applicable) was carried out and the F statistic was applied to check whether the nonsignificant terms can be omitted or not, from the full model. Tables 4.6 to 4.7 show results of analysis of variance of full and reduced model for PS and %EE of TMD NPs and Tables 4.8 to 4.9 show the results for LTG NPs.

Desirability

For simultaneous optimization of PS and EE desirability function (multi-response optimization techniques) was applied and total desirability was calculated using Design Expert software. The desirability lies between 0 and 1 and it represents the closeness of a response to its ideal value. The total desirability is defined as a geometric mean of the individual desirability for PS and EE (Derringer G and Suich R, 1980).

$$D = (d_{PS} \times d_{EE})^{1/2} \quad (2)$$

Where, D is the total desirability, and d_{PS} and d_{EE} are individual desirability for PS and EE. If both of the quality characteristics reach their ideal values, the individual desirability is 1 for both. Consequently, the total desirability is also 1.

4.2.1.2.3 Contour Plots

Two dimensional contour plots were established using reduced polynomial equation. At fixed levels of -1, 0 and 1 of independent variable with lowest coefficient value, values of other independent variables were computed for PS and entrapment efficiency and contour plots were established. Values of X_2 and X_3 were computed at prefixed values of PS & PDE. Three contour plots for both PS & PDE were established between X_2 and X_3 at fixed level of -1, 0 and 1 of X_1 as shown in Fig. 4.4 A-C & Fig. 4.6 A-C.

Check Point Analysis

A check point analysis was performed to confirm the utility of established contour plots and reduced polynomial equation in the preparation of TMD and LTG NPs. Values of two independent variables were taken from three check points each on contour plots plotted at fixed levels i.e. -1, 0 and 1 of independent variable of highest coefficient and the values of PS and EE were generated by NCSS software. NPs were prepared experimentally by taking the amounts of the independent variables on the same check points. Each batch was prepared in triplicate and mean values were determined and tabulated in Table 4.10 and 4.11 for TMD-NPs and LTG-NPs respectively. Difference of theoretically computed values of PS and entrapment efficiency and the mean values of experimentally obtained PS and entrapment efficiency were compared by using student't' test method.

4.2.1.2.4 Response Surface Plots

Response surface plots (Box GEP and Wilson KB, 1951; Kenneth WY et al., 1995) as a function of two factors at a time maintaining all other factors at fixed levels are more helpful in understanding both the main and the interaction effects of these two variables. These plots

can be easily obtained by calculating from the model, the values taken by one factor where the second varies (from -1 to 1 for instance) with constraint of a given Y value. The yield values for different levels of variables can also be predicted from the respective response surface plots depicted in Fig. 4.5A-C and Fig. 4.5D-E respectively for PS and EE of TMD-NPs. Similarly, Fig. 4.7 A-C and Fig. 4.7 D-E demonstrated response surface plots for LTG-NPs.

4.2.2 Transferrin and Lactoferrin conjugation of Nanoparticles

Transferrin (Tf) or Lamotrigine (Lf) was conjugated to the surface of the PLGA NPs by using a two step process as described by (Sahoo SK et al., 2004). Tf/Lf was conjugated to the hydroxyl group of surface cross linked PVA.

Figure 4.2: Schematic diagram of conjugation of Tf/Lf to NPs surface

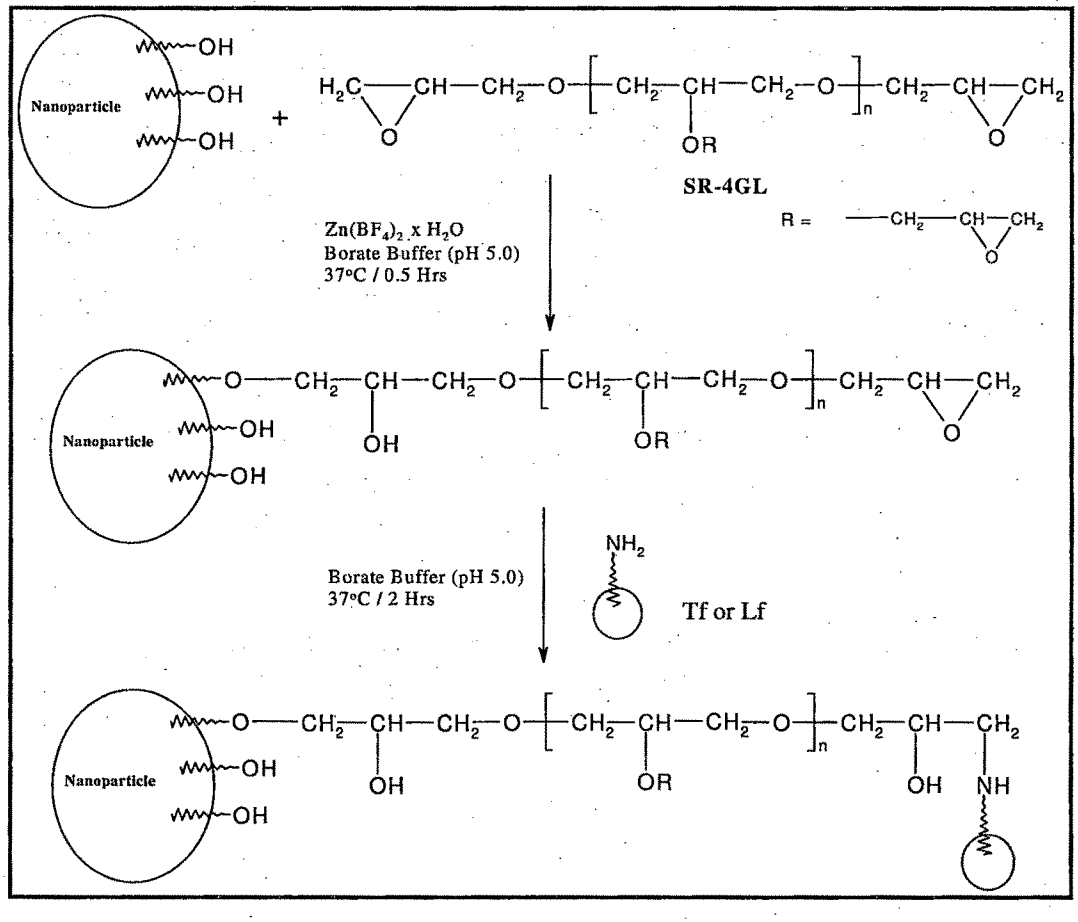

4.2.2.1 Conjugation procedure

Conjugation of Tf or Lf to the TMD-NPs surface was carried out by a two-step procedure with as described by Sahoo SK and Labhasetwar V (2005). The method involves the activation of NPs (75 mg) with an epoxy compound followed by the conjugation of Tf or Lf to the activated NPs. In the first step, the NP were dispersed in borate buffer (pH 5.0, 50 mM), then zinc tetrafluoroborate hydrate (10 mg) as a catalyst and a solution of SR-4GL as a linker were added. The reaction mixture was stirred on a magnetic stirrer at 37 °C for 30 min. The NPs were centrifuged at 20,000 rpm for 30 min at 4 °C and were washed twice with borate buffer to remove unreacted SR-4GL. In the second step, Tf or Lf in borate buffer was added in dispersion of the epoxy-activated NPs and the reaction mixture was stirred on magnetic stirrer at 37 °C for 2 h. The NPs were centrifuged at 20,000 rpm for 30 min at 4 °C to remove unreacted Tf. The NPs were washed twice with borate buffer and were stored at -40°C for 48h followed by lyophilization under vaccum at pressure less than 100 milli-torr.

4.2.2.2 Estimation of surface Transferrin/Lactoferrin density

The amount of the Tf and Lf conjugated to the surface of NPs was estimated using the BCA protein estimation kit (Genei, Bangalore). The NPs were centrifuged at 25,000 rpm for 30 min and supernatant was estimated for Tf and Lf. The actual conjugation was obtained in ug/mg of NPs as difference between total amount added and amount present in supernatant. NPs were centrifuged at 25000 rpm for 30 min and supernatant was separated. To 0.2 ml of the supernatant, 2 ml of the BWR (BCA working reagent) and incubated at 60°C for 30 min. The sample was allowed cool down to room temperature and the absorbance measured at 562 nm against a water reference treated in the similar manner as a blank. Test concentration was obtained from standard curve prepared by plotting the absorbance reading for standards (i.e. known concentrations). Amount of Tf/Lf measured in the supernatant and the washings was subtracted from the amount of Tf/Lf taken for conjugation. The amount of transferrin conjugated to the surface of the NPs was reported as amount of the Tf conjugated per mg of the NPs taken for conjugation.

4.2.2.3 Influence of amount of activating agent [Epoxy compound: SR-4GL]

The influence of the amount of activating agent (SR-4GL) on the surface Tf density and PS was checked by varying the amount of SR-4GL, keeping the weight of NPs (75 mg), catalyst (10 mg) and the amount of Tf/Lf taken for conjugation (1 mg) constant. The results for both TMD and LTG NPs are recorded in Table 4.12 and 4.14 respectively. Graphical

representation of the results for TMD-NPs and LTG-NPs are shown in Fig. 4.10 and 4.12 respectively.

4.2.2.4 Influence of amount of Transferrin and Lactoferrin

Influence of amount of Tf/Lf (taken for conjugation) on surface Tf/Lf density and PS was checked by varying the amount of Tf/Lf added to 75 mg of activated NPs, keeping optimized amount of SR-4GL constant. The results for both TMD-NPs and LTG-NPs are recorded in Table 4.13 and 4.15 respectively. Graphical representa and LTG-NPs are shown in Fig. 4.11 and 4.13 respectively.

4.2.2.5 [^{1}H]NMR of the Transferrin/Lactoferrin conjugated Nanoparticles

^{1}H-NMR spectroscopy was used to ascertain the conjugation of Tf/Lf to the NPs. The ^{1}H-NMR spectra of Tf-TMD-NPs, Lf-TMD-NPs and Tf-LTG-NPs, Lf-LTG-NPs are shown in Fig 4.14 and 4.15 respectively.

4.2.3 Lyophilization and optimization of lyoprotectant concentration

The optimization was performed on unconjugated NPs and effect of optimized lyoprotectant was confirmed for TF/Lf conjugated NPs. NPs were freeze-dried using different lyoprotectants such as sucrose, mannitol and trehalose to study their effect on change in PS and redispersibility of the unconjugated NPs. The redispersibility and PS of the NPs before and after freeze drying were evaluated. In order to determine the exact solid content of the NPs suspension, an aliquot suspension was first freeze-dried without lyoprotectant and the amount of NPs was determined by gravimetry. The amounts of lyoprotectant added to the nano particulate dispersions ranged from 1:0 to 1:2 (NPs:Lyoprotectant) of TMD-NPs as described in Table 4.16. Samples were frozen at −60 °C and lyophilization was carried out in a freeze drier for 48 h [Hetro Drywinner, Denmark]. Effect of optimized lyoprotectant on PS, redispersibility and aggregation behavior of conjugated NPs was tabulated in Table 4.17. Effect of different lyoprotectants and its concentration on the PS and redispersibilty of TMD-NPs is graphically represented in Fig. 4.16.

4.2.4 Characterization of Nanoparticles

The characterization of NPs is essential before proceeding for the *in vivo* studies. The characterization is performed for predicting the reproducible characteristics of the prepared NP formulation. The optimized NPs were characterized for PS, ZP, drug EE, *in vitro* drug

release, surface morphology, DSC and hydrophilicity. Various techniques for characterization of NPs include:

- Photon correlation spectroscopy (PCS) based on the dynamic light scattering (DLS) for PS or globule size and its distribution.
- The surface characteristic like charge is examined by measurement of ZP, surface morphology by transmission electron microscopy (TEM).
- The amount of the drug present in the NPs can be estimated by evaluation of the entrapment efficiency and is estimated by well known techniques of spectrophotometry.
- The *in vitro* release of the drug from the NPs influences the *in vivo* pharmacokinetic and pharmacodynamic behavior and is estimated by spectrophotometric method.
- Differential scanning calorimetry (DSC) is used for thermal characteristics of NPs, to determine the crystalline or amorphous nature of the ingredients or entire formulation.
- The surface hydrophilicity of the NPs influences the cellular uptake and also the *in vivo* pharmacokinetic behavior of the NPs. (Sahoo SK et al., 2002) PVA was determined using colorimetric iodine reaction and estimated spectrophotometrically (Joshi DP et al., 1979).

4.2.4.1 Particle size and Zeta potential determination

The PS and size distribution of drug loded NPs were determined using Photon Correlation Spectroscopy (PCS) technique. The PS was measured by Zetasizer (Malvern Instruments, Worcestershire, UK). The instrument is based on the principle of dynamic light scattering (DLS), also sometimes referred to as photon correlation spectroscopy (PCS) or quasi elastic light scattering. DLS is a technique of measuring the size of particles typically in the sub-micron region and is usually applied to the measurement of particle suspended within a liquid. The technique measures particle diffusion due to Brownian motion and relates this to the size of the particles. Brownian motion is the random movement of particles due to the bombardment by the solvent molecules that surrounds them. The parameter calculated is defined as the translational diffusion coefficient. The PS is then calculated from the translational diffusion coefficient using the Strokes-Einstein equation.

Malvern Zetasizer nano ZS was used to measure the ZP of the particles based on the electrophoresis and electrical conductivity of the prepared NPs. The electrophoretic mobility (μm/s) of the particles was converted to the ZP by in-built software based on Helmholtz-Smoluchowski equation. Measurements were performed using small volume disposable zeta cell. Dilute suspension (10 times) of NPs was prepared in distilled water and was subjected to PS analysis and ZP measurement. The observations for TMD and LTG are tabulated in Table 4.18.

4.2.4.2 Drug entrapment efficiency

To determine entrapment efficiency, percentage amount of drug entrapped in the NPs, 2 mg of NPs were added to acetonitrile and subjected to shaking at room temperature, for extraction of drug from the NPs, using cyclomixer. The resulting solution was centrifuged at 10,000 rpm for 15 mins to remove the precipitated components. The supernatant was further diluted with acetonitrile and estimated using UV spectrophotometry. The amount of drug in NPs was determined by spectrophotometrically. The percentage drug entrapment efficiency (EE) was calculated using the following expression.

% EE = (Amount of drug in NPs/Amount of drug added in formulation) × 100

The results are recorded in Table 4.18.

4.2.4.3 Transmission electron microscopy

NPs were dispersed in de-ionized water at a concentration of 1mg/ml. To measure the morphology and size distribution of NPs, a drop of sample was placed onto a 300-mesh copper grid coated with carbon. Approximately 2 min after deposition, the grid was tapped with filter paper to remove surface water and air-dried. Negative staining was performed using a droplet of 0.5 % w/v phosphotungstic acid. Transmisssion electron microscopy was performed using Morgagni 268, Philips (Netherlands) transmission electron microscope. The TEM images for unconjugated and conjugated NPs for TMD and LTG are shown in Fig. 4.17 (A, B, C) and 4.18 (A, B, C) respectively.

4.2.4.4 Differential Scanning Calorimetry

DSC analysis was carried out for TMD, PLGA, PVA, TMD-NPs, LTG, LTG-NPs using a Differential scanning calorimeter (Mettler Toledo DSC, Japan). An empty aluminium pan was used as the reference for all measurements. During each scan, 3-5 mg of sample was heated, in a hermetically sealed aluminium pan, at a heating rate of 10° C/min, from 30°C to

280°C, under inert nitrogen atmosphere at a flow rate of 40 ml/min. DSC thermograms were recorded using Mettler Toledo Star SW 7.01 software. Fig. 4.19 shows the thermograms of TMD-NPs, TMD, PLGA, PVA. Fig. 4.20 shows the thermograms of LTG-NPs, LTG, PLGA, PVA.

4.2.4.5 *In vitro* drug release

The *in vitro* drug release of TMD and LTG loaded NPs was carried out at 37°C, in Phosphate buffer saline (PBS) pH 7.4 with 2% Tween 80 and PBS pH 7.4 with 1% SLS respectively as dissolution media. NPs equivalent to 2 mg drug were suspended in 20 ml of dissolution media in screw capped tubes, which were placed in a horizontal shaker bath maintained at 37°C and shaken at 60 per min., Samples were taken out at specific time intervals and centrifuged at 25,000 rpm for 30 min. The residue (settled NPs) was collected and drug remaining in the NPs after release was measured using UV spectrophotometer by dissolving in acetonitrile. The concentration of drug was determined spectrophotometrically. The amount of the drug released was calculated using the following equation:

Cumulative % drug released = 100 - % drug Remaining

$$\% \text{ Drug remaining} = \left(\frac{\text{Amount of drug in the NPs settled}}{\text{Initial amount of drug in NPs}}\right) \times 100$$

The release of drug from the unconjugated and conjugated NPs of TMD and LTG is shown in Fig. 4.21 and 4.22 respectively.

4.2.4.6 Estimation of residual PVA in Nanoparticles

The amount of residual PVA associated with NPs was determined by a colorimetric method based upon the formation of a colored complex between two adjacent hydroxyl groups of PVA and an iodine molecule (Joshi DP et al., 1979). Briefly, 2 mg of NPs sample was treated with 2 ml of 0.5 M NaOH for 15 min at 60 °C. Each sample was neutralized with 900 µl of 1 N HCl and the volume was adjusted to 5 ml with distilled water. To each sample, 3 ml of a 0.65 M solution of boric acid, 0.5 ml of a solution of I_2/KI (0.05 M/0.15 M), and 1.5 ml of distilled water were added. Finally, the absorbance of the samples was measured at 690 nm after 15 min incubation. Residual PVA was determined using standard plot of PVA (chapter 3, section 3.4.3).

4.3 Results and Discussion

4.3.1 Preparation and optimization of Nanoparticles

The nanoprecipitation method developed by Fessi et al., represents an easy and reproducible technique and very often used to prepare NPs from PLGA polymer.

Figure 4.3: Schematic diagram for the method of preparation of NPs

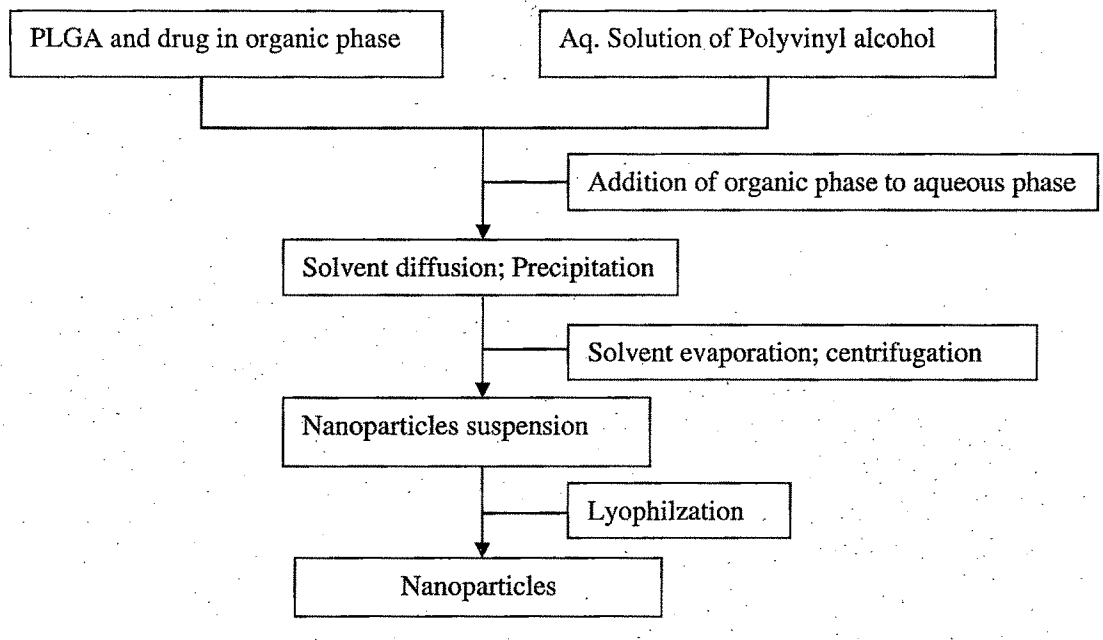

4.3.1.1 Preliminary optimization of various formulation parameters

4.3.1.1.1 Selection of organic phase

Acetone gave particles with higher percentage TMD entrapment compared to acetonitrile and THF as shown in Table 4. Although PS was slightly higher with acetone compared to acetonitrile, based on the PDE, acetone was selected as a solvent for the NPs preparation. NPs obtained using acetonitrile were slightly smaller than the NPs obtained by using acetone/THF. This could be because acetonitrile has greater water miscibility than acetone/THF (Technical Bulletin K0520, Wiley interscience, 2002) which may lead to instant precipitation of NPs as compared to acetone/THF. However, entrapment efficiency of NPs reduced considerably when acetonitrile and THF were used as solvents. Reduction in entrapment efficiency could be due to higher boiling point of acetonitrile & THF (www.jtbaker.com) and slower evaporation rate (Technical Bulletin K0520, Wiley interscience, 2002) as compared to acetone, which may lead to leaching of the drug during solvent evaporation. Same system was employed for other drug LTG.

Table 4.3: Selection of Organic Phase

Solvent	PS ± SD* (nm)	EE ± SD* (%)
Acetone	189.0 ± 9.5	60.3 ± 1.6
Acetonitrile	164.7 ± 7.8	46.7 ± 1.1
Tetrahydrofuran	278.6 ± 14.3	29.6 ± 1.3

* n=3

4.3.1.1.2 Optimization of process parameters

The process parameters such as the stirrer speed and rate of addition of organic phase affect the formation of the NPs. As commonly reported in the literature (Fessi H et al., 1989, Derakhshandeh K et al., 2007) the rate of addition of the organic phase to the aqueous phase was kept constant at 0.5ml/min. The speed of stirring was evaluated for the formation of NPs. The process was executed at slow, moderate and high speed of the stirrer and the observations are made. At moderate speed of the stirrer there was uniform NPs dispersion with no particle aggregation. However, at slow speed the vortex formation was inadequate and hence leads to the deposition of the solids at the surface of the aqueous phase. At high stirrer speed there was aggregation of the NPs. This may be due to the high shear causing insufficient stabilization of NPs and causing particle aggregation. Hence the all the batches further were prepared at the moderate speed of the stirrer.

4.3.1.2 Factorial design and optimization of Nanoparticles

In this study, the main parameters affecting the NPs formulation were found to be %w/v PVA concentration in aqueous phase, polymer concentration (keeping the amount of the drug constant) and the ratio of the organic: aqueous phase (represented in decimal form). Hence, polymer concentration, %w/v PVA concentration and organic: aqueous phase ratio were selected as independent variables to find the optimized condition for small PS (PS) (< 150 nm) and highest % drug entrapment efficiency (EE) using 3^3 factorial design and the results are recorded in Table 4.4 and 4.5 for TMD and LTG respectively.

For intravenous administration, PS < 200nm is preferred to prevent opsonization [S.M. Moghimi, 1993]. In this study, the drug loaded PLGA NPs were to be surface conjugated with ligand further. Hence the optimization criteria for PS of drug loaded NPs was kept as < 150 nm with highest drug entrapment efficiency.

Twenty-seven batches for each of TMD and LTG NPs were prepared by nanoprecipitation method using 3^3 factorial design (Table 4.3) varying three independent variables namely %w/v PVA concentration (X_1), polymer concentration (X_2) & organic: aqueous phase ratio (X_3). The influence of these independent variables on the dependent variables PS (PS) and % drug entrapment efficiency (%EE) was evaluated. The results for TMD NPs are recorded in Table 4.4 and for LTG in Table 4.5.

Table 4.4: 3^3 factorial experimental design for TMD-NPs

Batch	X_1	X_2	X_3	PS (±SD) nm	EE (±SD) %
1	-1	-1	-1	154.8(4.8)	60.28(1.8)
2	-1	-1	0	139.5(5.8)	56.49(2.1)
3	-1	-1	1	124.1(5.1)	55.06(1.4)
4	-1	0	-1	169.9(3.5)	69.91(1.6)
5	-1	0	0	159.1(4.3)	68.36(1.5)
6	-1	0	1	140.5(4.4)	64.97(2.0)
7	-1	1	-1	185.3(6.2)	78.35(1.3)
8	-1	1	0	167.6(4.5)	76.86(2.2)
9	-1	1	1	155.1(3.8)	74.40(0.6)
10	0	-1	-1	143.6(5.2)	57.96(1.7)
11	0	-1	0	128.9(4.9)	54.45(2.3)
12	0	-1	1	114.9(4.6)	52.83(1.5)
13	0	0	-1	156.6(5.4)	69.16(1.4)
14	0	0	0	144.5(3.7)	66.15(1.4)
15	0	0	1	129.2(5.5)	64.52(1.8)
16	0	1	-1	170.1(4.1)	77.90(1.9)
17	0	1	0	157.7(4.1)	75.74(1.1)
18	**0**	**1**	**1**	**141.1(3.7)**	**73.57(2.1)**
19	1	-1	-1	139.2(3.4)	54.42(1.7)
20	1	-1	0	121.9(3.0)	51.37(1.9)
21	1	-1	1	108.6(3.5)	49.23(1.8)
22	1	0	-1	153.2(2.8)	66.01(2.2)
23	1	0	0	142.8(4.2)	62.82(2.3)
24	1	0	1	124.3(3.7)	61.32(1.9)
25	1	1	-1	166.0(2.9)	74.05(1.7)
26	1	1	0	152.1(3.0)	71.42(0.9)
27	1	1	1	134.9(3.9)	68.85(1.1)

Values are represented as mean ± SD, n=3

Table 4.5: 3^3 factorial experimental design for LTG-NPs

Batch	X_1	X_2	X_3	PS (±SD) nm	EE (±SD) %
1	-1	-1	-1	142.7(4.4)	64.14(1.5)
2	-1	-1	0	128.6(3.4)	60.10(1.8)
3	-1	-1	1	114.3(3.9)	58.59(1.9)
4	-1	0	-1	156.6(5.0)	74.38(2.0)
5	-1	0	0	146.7(4.7)	72.74(1.6)
6	-1	0	1	129.5(4.1)	69.13(1.3)
7	-1	1	-1	170.7(6.3)	83.36(1.8)
8	-1	1	0	154.4(4.0)	81.78(1.5)
9	-1	1	1	143.0(4.1)	79.17(1.9)
10	0	-1	-1	136.3(3.7)	61.67(1.3)
11	0	-1	0	122.3(3.2)	57.93(2.0)
12	0	-1	1	109.1(5.3)	56.21(1.2)
13	0	0	-1	148.6(3.6)	73.59(2.1)
14	0	0	0	137.2(5.6)	70.38(1.9)
15	0	0	1	122.7(4.3)	68.65(1.7)
16	0	1	-1	161.5(3.4)	81.78(1.1)
17	0	1	0	149.7(3.2)	80.59(1.8)
18	**0**	**1**	**1**	**133.9(3.6)**	**78.28(1.7)**
19	1	-1	-1	129.5(2.9)	57.90(2.1)
20	1	-1	0	113.4(4.9)	54.66(0.9)
21	1	-1	1	101.0(3.1)	52.39(1.4)
22	1	0	-1	142.6(4.5)	70.24(1.2)
23	1	0	0	132.9(3.0)	66.84(1.5)
24	1	0	1	115.7(4.7)	65.25(1.5)
25	1	1	-1	154.5(4.0)	78.80(2.4)
26	1	1	0	141.6(6.2)	75.99(1.2)
27	1	1	1	125.5(3.5)	73.26(1.6)

Values are represented as mean ± SD, n=3

Multiple Regression Analysis

A full model was established after putting the values of regression coefficients in Equation 1. Equations 3 and 4 represent the full model equations for TMD-NPs for PS and entrapment efficiency respectively.

$$Y_{PS} = 144.87 - 8.49X_1 + 14.13X_2 - 14.78X_3 + 3.65X_1^2 - 1.93X_2^2 - 0.93X_3^2 - 0.52X_1X_2 - 0.02X_1X_3 - 0.03X_2X_3 - 0.12X_1X_2X_3 \quad (3)$$

$$Y_{EE} = Y = 66.47 - 2.51X_1 + 9.95X_2 - 2.41X_3 - 1.13X_1^2 - 1.29X_2^2 + 0.3X_3^2 + 0.13X_1X_2 - 0.08X_1X_3 + 0.17X_2X_3 - 0.16X_1X_2X_3 \quad (4)$$

Equation 5 and 6 represent the full model equations for LTG-NPs for PS and entrapment efficiency respectively.

$$Y_{PS} = 137.51 - 7.22X_1 + 13.20X_2 - 13.80X_3 + 0.03X_1^2 - 1.82X_2^2 - 0.89X_3^2 - 0.40X_1X_2 - 0.11X_1X_3 - 0.02X_2X_3 - 0.15X_1X_2X_3 \quad (5)$$

$$Y_{EE} = Y = 70.68 - 2.67X_1 + 10.52\ X_2 - 2.50X_3 - 1.08X_1^2 - 1.43X_2^2 + 0.27X_3^2 + 0.14X_1X_2 - 0.09\ X_1X_3 + 0.27X_2X_3 - 0.17X_1X_2X_3 \quad (6)$$

Neglecting nonsignificant ($P > 0.05$) terms from the full model, a reduced model was established, which facilitates the optimization technique by plotting contour plots keeping one major contributing independent formulation variable constant and varying other two independent formulation variables to establish the relationship between independent and dependent variables.

Equations 6 and 7 represent the reduced model equations for TMD-NPs for PS and entrapment efficiency respectively.

$$Y_{PS} = 142.96 - 8.49X_1 + 14.13X_2 - 14.78X_3 + 3.65X_1^2 \quad (7)$$

$$Y_{EE} = 66.67 - 2.51X_1 + 9.95\ X_2 - 2.41X_3 - 1.13X_1^2 - 1.29X_2^2 \quad (8)$$

Equation 8 and 9 represent the reduced model equations for LTG-NPs for PS and entrapment efficiency respectively.

$$Y_{PS} = 135.72 - 7.21X_1 + 13.20X_2 - 13.88X_3 \quad (9)$$

$$Y_{EE} = 70.85 - 2.67X_1 + 10.52\ X_2 - 2.49X_3 - 1.08X_1^2 - 1.43X_2^2 \quad (10)$$

The PS and %EE obtained at various levels of three independent variables (X_1, X_2 and X_3) were subjected to multiple regression. Second order polynomial equations (full model) were obtained. The effects of X_1, X_2 and X_3 on PS and % EE were evaluated by changing one variable at a time from its low to high value. The interactions (X_1X_2, X_1X_3, X_2X_3 and $X_1X_2X_3$) show how the PS and entrapment efficiency changes when two or more variables were simultaneously changed.

Table: 4.6: Analysis of Variance of PS for Full and Reduced Model for TMD-NPs

		df	SS	MS	F	R^2
Regression	FM	10	8936.245	893.625	332.192	0.995
	RM	4	8905.144	2226.286	660.599	0.992
Error	FM	16	43.041(E1)	2.690		
	RM	22	74.142(E2)	3.370		

FM, full model; RM, reduced model; df, Degree of freedom; SS, Sum of squares; MS, Mean squares; F, Fischer ratio; E1 and E2, Sum of squares of error of full and reduced model respectively.
Number of parameters omitted (N) = 4
F calculated = [(SSE2 – SSE1)/N]/ MS of error for FM = 1.93
F tabulated = 2.74 (α = 0.05, V1 = 6, and V2 = 16)

Table 4.7: Analysis of Variance of EE for Full and Reduced Model TMD-NPs

		Df	SS	MS	F	R^2
Regression	FM	10	2017.673	201.767	634.457	0.997
	RM	5	2016.290	403.258	1308.526	0.997
Error	FM	16	5.088(E1)	0.318		
	RM	21	6.472(E2)	0.308		

FM, full model; RM, reduced model; df, Degree of freedom; SS, Sum of squares; MS, Mean squares; F, Fischer ratio; E1 and E2, Sum of squares of error of full and reduced model respectively.
Number of parameters omitted (N) = 5
F calculated = [(SSE2 – SSE1)/N]/ MS of error for FM = 0.87
F tabulated = 2.85 (α = 0.05, V1 = 5, and V2 = 16)

Table 4.8: Analysis of Variance of PS for Full and Reduced Model for LTG-NPs

		Df	SS	MS	F	R^2
Regression	FM	10	7582.598	752.860	348.312	0.995
	RM	3	7501.685	2500.561	935.234	0.992
Error	FM	16	34.583(E1)	2.161		
	RM	23	61.496(E2)	2.674		

FM, full model; RM, reduced model; df, Degree of freedom; SS, Sum of squares; MS, Mean squares; F, Fischer ratio; E1 and E2, Sum of squares of error of full and reduced model respectively.
Number of parameters omitted (N) = 7
F calculated = [(SSE2 – SSE1)/N]/ MS of error for FM = 1.78
F tabulated = 2.66 (α = 0.05, V1 = 7, and V2 = 16)

For TMD-NPs, the PS and entrapment values for the 27 batches showed a wide variation starting from a minimum of 108.6 nm to maximum of 185.3 nm and minimum of 49.2 % to maximum of 78.3 % respectively as shown in Table 4.4. The coefficients of terms X_2^2, X_3^2, X_1X_2, X_2X_3, X1X3 and $X_1X_2X_3$ ($p>0.05$) in equation 3 are regarded as least contributing to the PS of TMD. Similarly, the coefficients of terms X_3^2, X_1X_2, X_1X_3, X_2X_3 and $X_1X_2X_3$

(having p>0.05) in equation 4 are regarded as least contributing to the % EE of TMD. Hence, these terms were neglected from full model considering non-significant and reduced polynomial equation 7 and 8 were obtained for PS and %EE respectively by including significant terms (p<0.05) of equation 3 and 4 respectively.

Table 4.9: Analysis of Variance of EE for Full and Reduced Model LTG-NPs

		Df	SS	MS	F	R^2
Regression	FM	10	2255.001	225.500	597.521	0.997
	RM	5	2253.13	450.625	1195.786	0.997
Error	FM	16	6.038(E1)	0.377		
	RM	21	7.914(E2)	0.377		

FM, full model; RM, reduced model; df, Degree of freedom; SS, Sum of squares; MS, Mean squares; F, Fischer ratio; E1 and E2, Sum of squares of error of full and reduced model respectively.
Number of parameters omitted (N) = 5
F calculated = [(SSE2 – SSE1)/N]/ MS of error for FM = 0.99
F tabulated = 2.85 (α = 0.05, V1 = 5, and V2 = 16)

The goodness of fit of the model was checked by the determination coefficient (R^2). The determination coefficient, R^2 is a measure of the amount of reduction in the variability of Y obtained by using the regressor variables X_1, X_2, and X_3. As shown in Table 4.8 and Table 4.9, the high value of the determination coefficient R^2 for PS and EE indicated a high significance of the models. F-statistic of the results of ANOVA of full model and reduced model (as represented in Table 4.6 and 4.7) confirmed omission of non-significant terms of equation 3 and equation 4. Since Fcal (1.93) < Ftab (2.74) for PS and Fcal (0.87) < Ftab (2.85) for %EE, it was concluded that the neglected terms do not significantly contributing in predicting of PS and entrapment efficiency. For equation 7 and 8, sign of the coefficients explains the nature of effect while magnitudes determine extent of effect for variables. The equation shows quadratic term with sign different from the linear term (X_1^2 in Eq. 7 and X_2^2 in Eq. 8) however, in the concentration range tested the linear term overpower the quadratic term and thus decide the nature of effect. When the coefficient values of three independent key variables (X_1, X_2, & X_3) in equation 7 were compared ignoring the sign, the value for variable X_2 (b_1 = 14.13) and X_3 (b_2 = -14.78) were found to be higher and hence the variable polymer concentration (X_2) and Volume of organic phase (X_3) were considered to be a major contributing variable for PS. Similarly, when the coefficient values of three independent key variables (X_1, X_2, & X_3) in equation 8 were compared ignoring the sign, the value for variable X_2 (b_1 = 9.95) was found to be higher and hence the variable polymer concentration (X_2) considered to be a major contributing variable for EE.

For LTG-NPs, the PS and entrapment values for the 27 batches showed a wide variation starting from a minimum of 101.0 nm to maximum of 170.7 nm and minimum of 52.4 % to maximum of 83.4 % respectively as shown in Table 4.5. The coefficients of terms X_1^2, X_2^2, X_3^2, X_1X_2, X_2X_3, X_1X_3 and $X_1X_2X_3$ ($p>0.05$) in equation 2 are regarded as least contributing to the PS of LTG. Similarly, the coefficients of terms X_3^2, X_1X_2, X_1X_3, X_2X_3 and $X_1X_2X_3$ (having $p>0.05$) in equation 6 are regarded as least contributing to the %EE of LTG. Hence, these terms were neglected from full model considering non-significant and reduced polynomial equation 9 and 10 were obtained for PS and %EE respectively by including significant terms ($p<0.05$) of equation 3 and 4 respectively.

The goodness of fit of the model was checked by the determination coefficient (R^2). The determination coefficient, R^2 is a measure of the amount of reduction in the variability of Y obtained by using the regressor variables X_1, X_2, and X_3. As shown in Table 4.8 and 4.9, the high value of the determination coefficient R^2 for PS and EE indicated a high significance of the models. F-statistic of the results of ANOVA of full model and reduced model (as represented in Table 4.8 and 4.9) confirmed omission of non-significant terms of equation 5 and 6. Since Fcal (1.78) < Ftab (2.66) for PS and Fcal (0.99) < Ftab (2.85) for %EE, it was concluded that the neglected terms do not significantly contributing in predicting of PS and entrapment efficiency. For equation 9 and 10, sign of the coefficients explains the nature of effect while magnitudes determine extent of effect for variables. The equation shows quadratic term with sign different from the linear term (X_2^2 in Eq. 10) however, in the concentration range tested the linear term overpower the quadratic term and thus decide the nature of effect. When the coefficient values of three independent key variables (X_1, X_2, & X_3) in equation 9 were compared ignoring the sign, the value for variable X_2 ($b_1 = 13.20$) and X_3 ($b_2 = -13.88$) were found to be higher and hence the variable polymer concentration (X_2) and Volume of organic phase (X_3) were considered to be a major contributing variable for PS. Similarly, when the coefficient values of three independent key variables (X_1, X_2, & X_3) in equation 10 were compared ignoring the sign, the value for variable X_2 ($b_1 = 10.52$) was found to be higher and hence the variable polymer concentration (X_2) considered to be a major contributing variable for EE. The optimum formulation offered by software based on desirability was found at 0, 1, and 1 level of X_1, X_2, and X_3 respectively. The calculated desirability factor for offered formulations was 1.00 indicating suitability of the designed factorial model.

Influence of the Polymer (PLGA) Concentration

The increase in the concentration of PLGA resulted in the increase in the PS of the NPs. The viscosity of PLGA appears to affect the size of NPs due to hindrance in rapid dispersion of PLGA solution of higher viscosity into the aqueous phase resulted in increase in the PS (Chorny M et al., 2002). Availability of PVA on the surface of NPs prevents the aggregation of NPs during solvent evaporation but in case of higher concentrations of PLGA, deposition of PVA on the particle surface may not be uniform and sufficient leading to increase in PS. However, increase in concentration of PLGA increases the EE. It may be due to increase in drug entrapping polymer and resultant decrease in the diffusion of the drug towards the aqueous phase (Xiangrong S et al., 2008a and 2008b). The increase in PS with the increasing PLGA concentration, can increase the length of diffusion pathways of drugs from the organic phase to the aqueous phase, thus reduce the drug loss through diffusion and increase EE.

Influence of PVA concentration

PS of NPs decreased with the increase of PVA concentration. With increase in concentration more PVA can be oriented at organic solvent/water interface thereby reducing interfacial tension efficiently (Galindo-Rodriguez Set al., 2004), which promoted the formation of smaller emulsion droplets. Also, with the increase in PVA concentration, the viscosity of the external aqueous phase increased, which resulted increase in size due to decrease in the net shear stress (Budhian A et al., 2005). However, the reduction of the interfacial tension dominates over increase in viscosity. Thus, at sufficient concentration, PVA cover the droplets completely and avoid coalescence of droplets during the removal of organic solvent thereby forming NPs with smaller size. In addition, a large number of hydroxyl groups extending into the continuous phase forms hydrated layer at the surface hinder NPs aggregation. The decrease in EE with the increase of PVA concentration was probably due to decrease in PS (Xiangrong S et al., 2008a).

Influence of the organic: aqueous phase ratio

The PS and EE were found to be inversely proportional to the organic: aqueous phase ratio. As the organic: aqueous phase ratio was increased, the PS and drug EE were decreased. The increase in the organic phase ratio leads to increased evaporation time causing slower polymer precipitation, and thereby formation of small particles. Due to the increased evaporation time and slower polymer precipitation, the tendency of the drug to escape in the aqueous phase before polymer precipitation increases, leading to lower drug EE.

Figure 4.4: Contour plots of TMD-NPs: Effect of polymer concentration (X_2) and volume of organic phase (X_3) on PS (PS) at -1 level of stabilizer concentration (X_1) (A), at 0 level of X_1 (B), at +1 level of X_1 (C); Effect of X_2 and X_3 on entrapment efficiency (EE) at -1 level of X_1 (D), at 0 level of X_1 (E), at +1 level of X_1 (F).

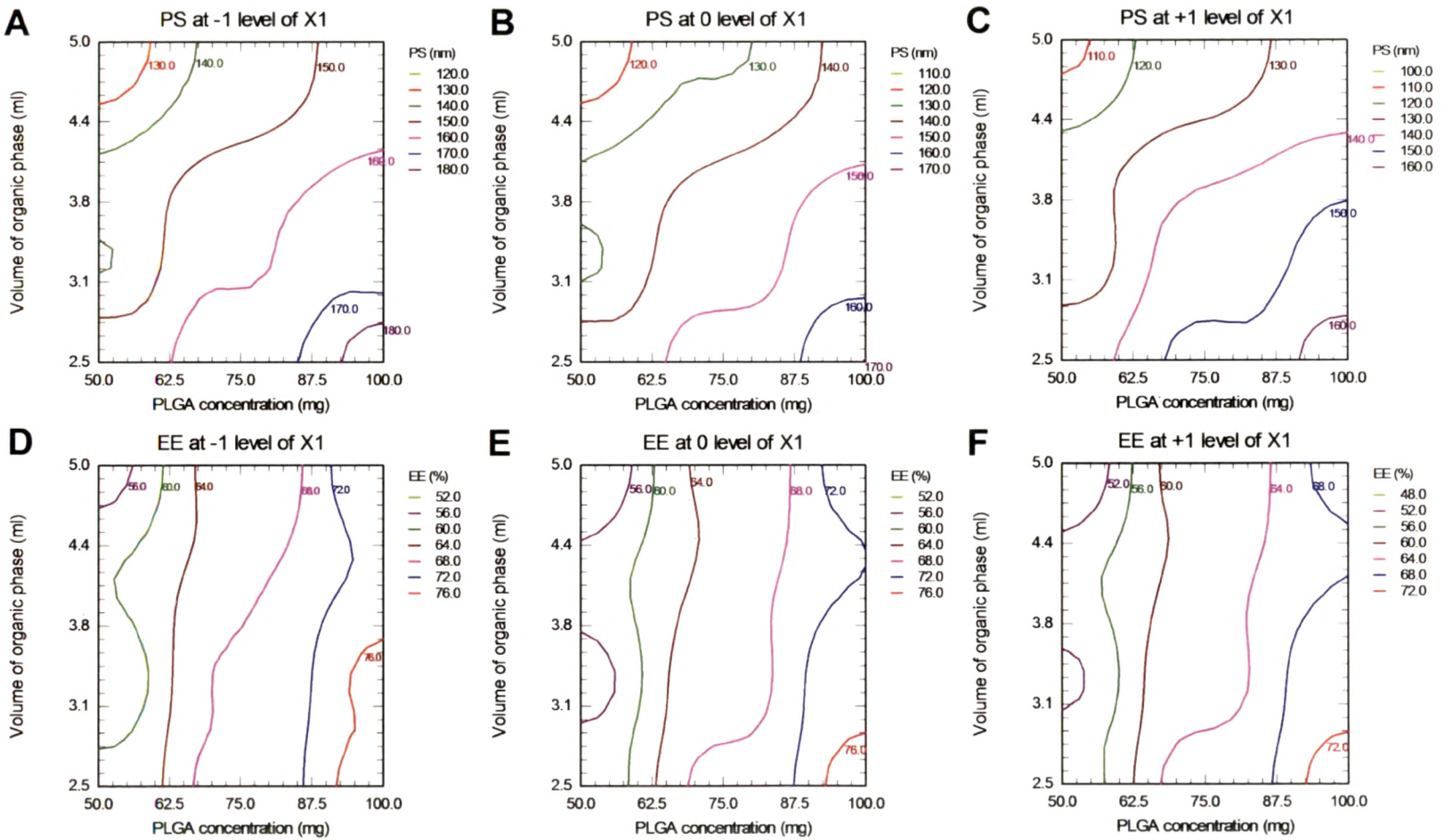

Figure 4.5: Response surface plots of TMD-NPs: Effect of polymer concentration (X_2) and volume of organic phase (X_3) on PS (PS) at -1 level of stabilizer concentration (X_1) (A), at 0 level of X_1 (B), at +1 level of X_1 (C); Effect of X_2 and X_3 on entrapment efficiency (EE) at -1 level of X_1 (D), at 0 level of X_1 (E), at +1 level of X_1 (F).

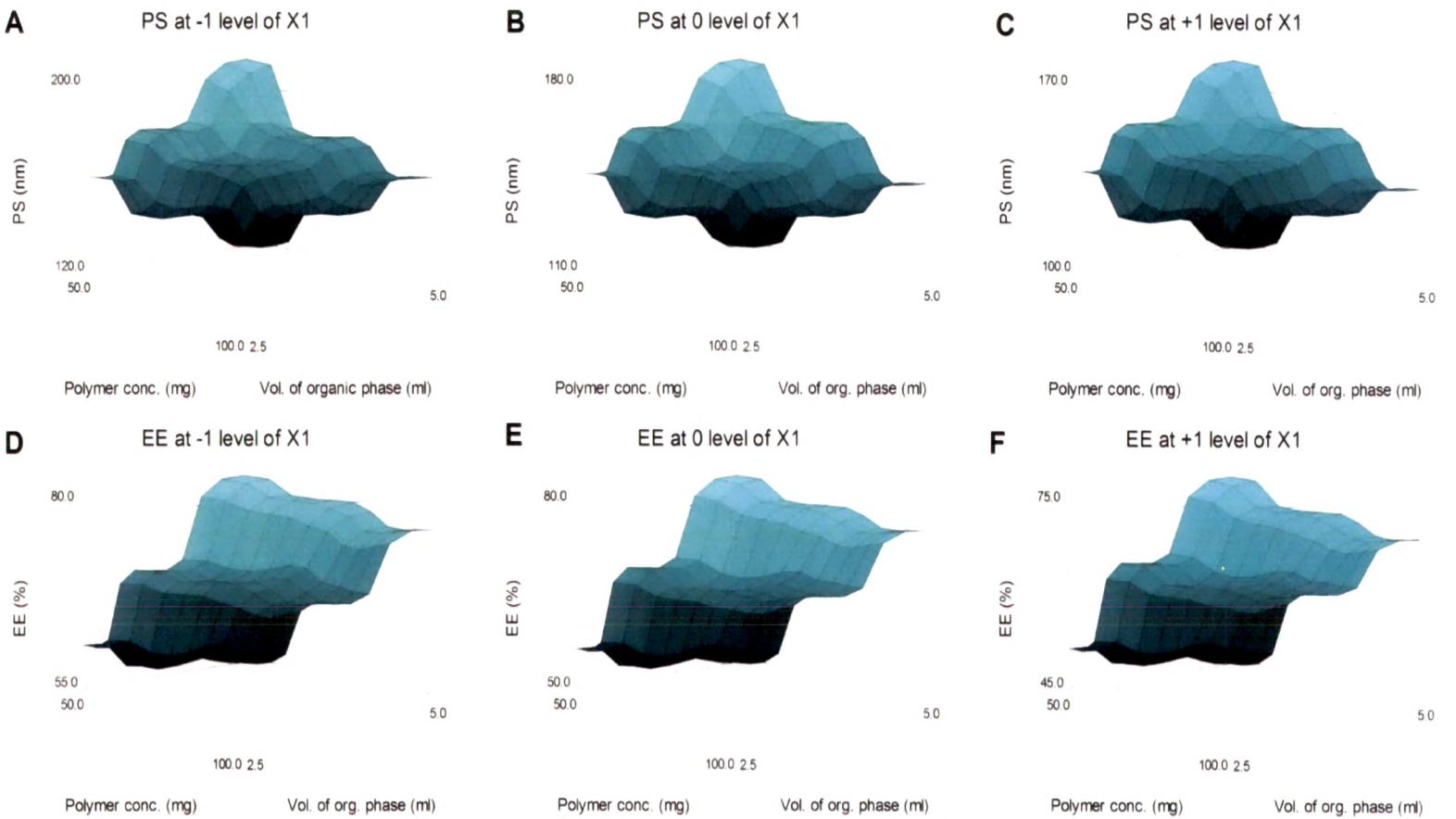

Figure 4.6: Contour plots of LTG-NPs: Effect of polymer concentration (X_2) and volume of organic phase (X_3) on PS (PS) at -1 level of stabilizer concentration (X_1) (A), at 0 level of X_1 (B), at +1 level of X_1 (C); Effect of X_2 and X_3 on entrapment efficiency (EE) at -1 level of X_1 (D), at 0 level of X_1 (E), at +1 level of X_1 (F).

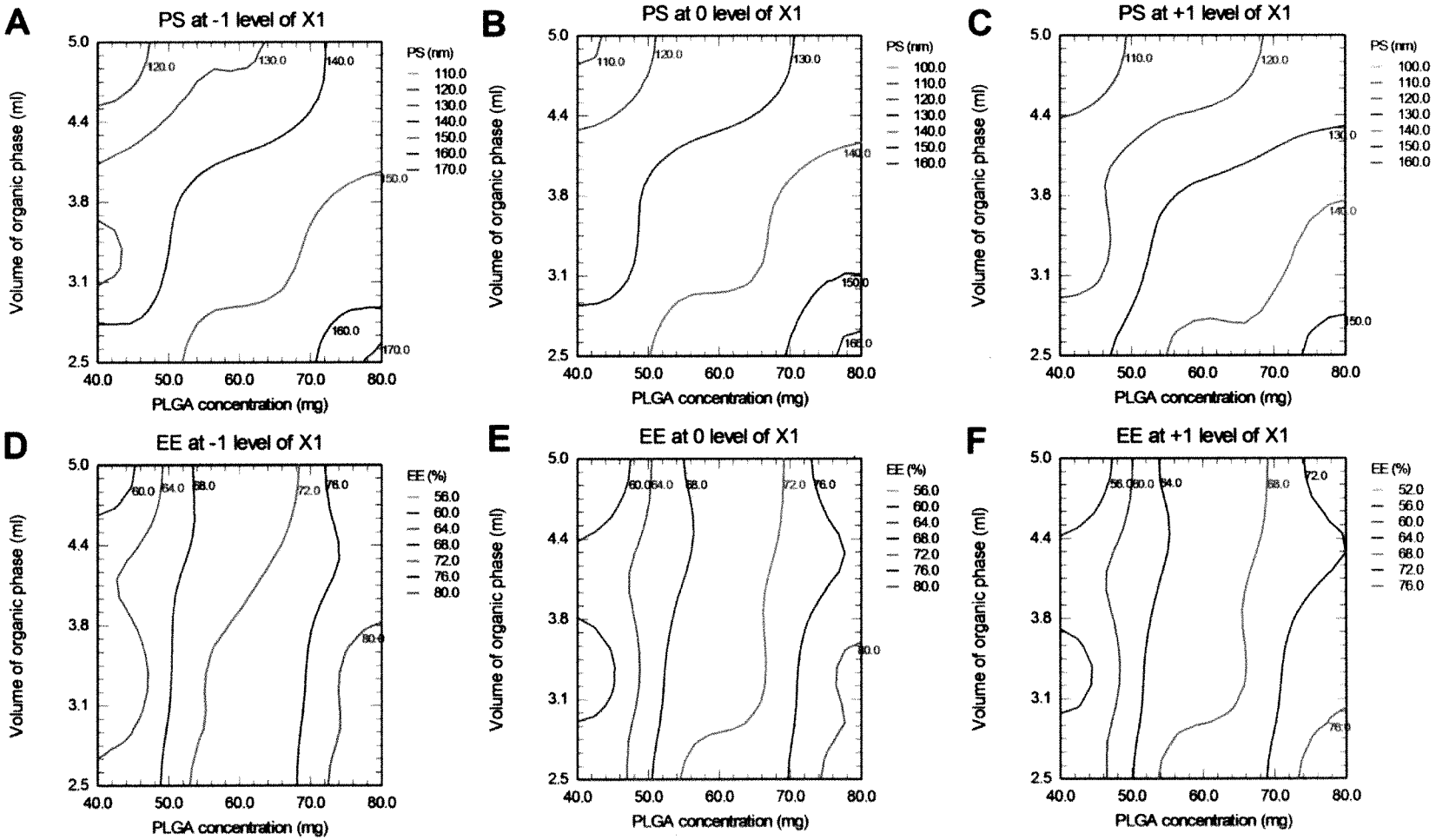

Figure 4.7: Response surface plots of LTG-NPs: Effect of polymer concentration (X_2) and volume of organic phase (X_3) on PS (PS) at -1 level of stabilizer concentration (X_1) (A), at 0 level of X_1 (B), at +1 level of X_1 (C); Effect of X_2 and X_3 on entrapment efficiency (EE) at -1 level of X_1 (D), at 0 level of X_1 (E), at +1 level of X_1 (F).

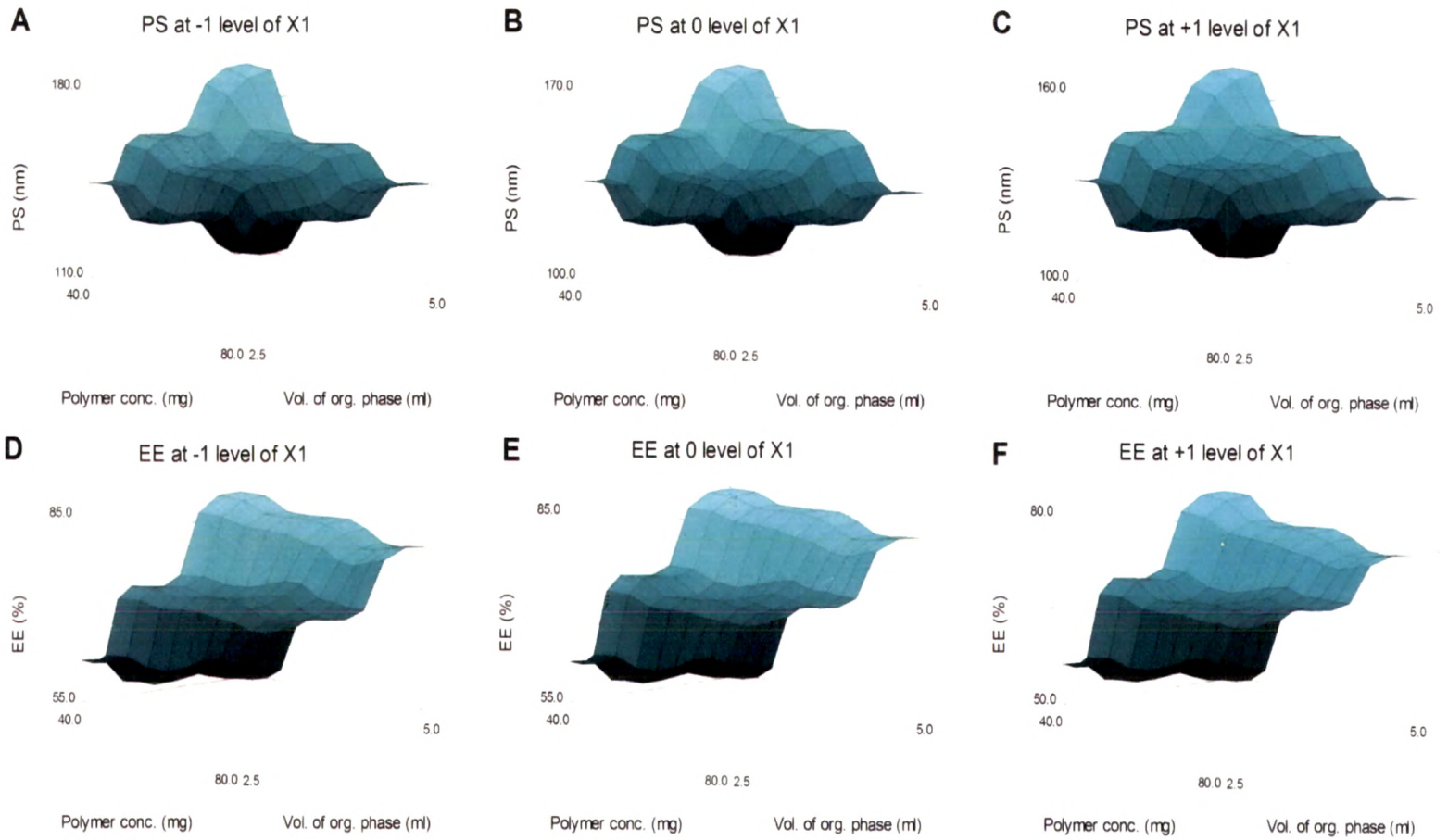

Figure 4.8: Overlay of contour plots of PS and EE for TMD-NPs at 0 level of stabilizer concentration (X_1)

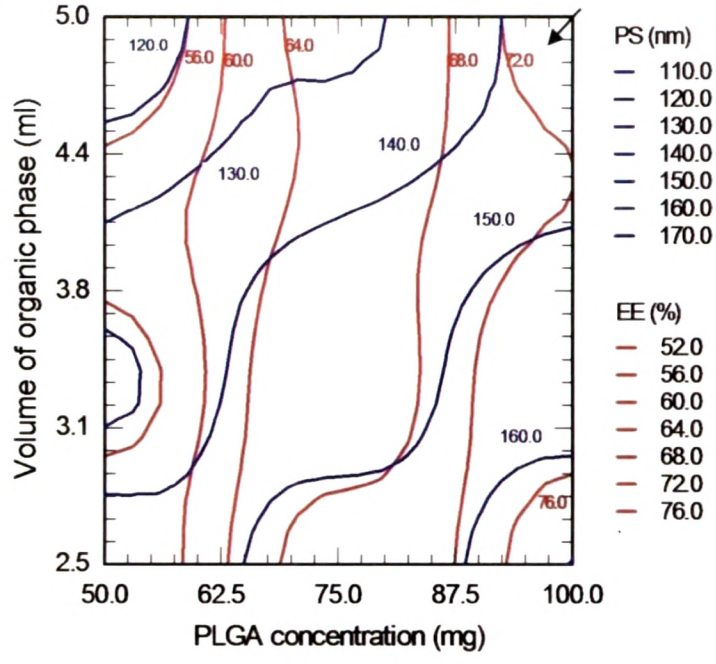

Figure 4.9: Overlay of contour plots of PS and EE for LTG-NPs at 0 level of stabilizer concentration (X_1)

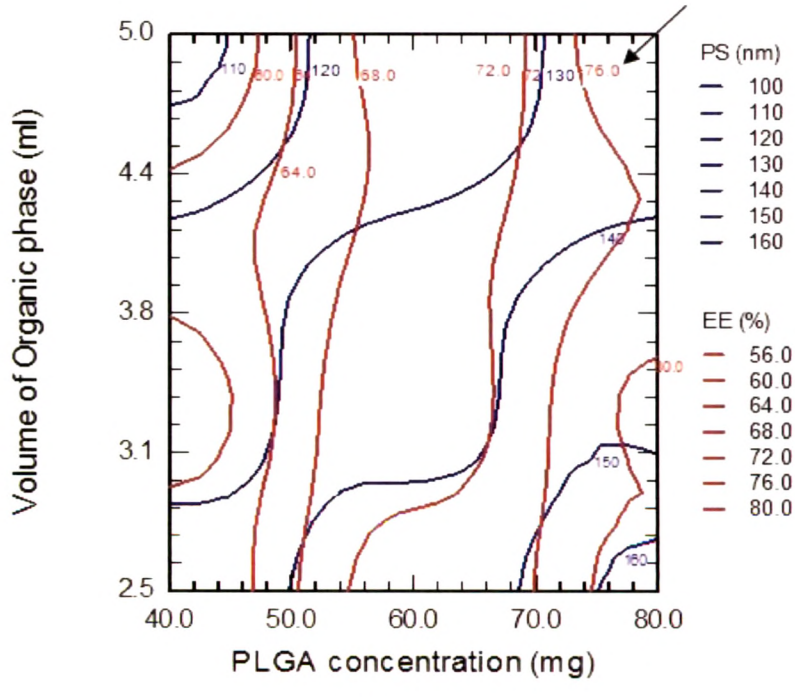

Contours Plots

Contour plots and response surface plots were employed as graphical representation of optimization process. The overlay of contours presents effective tool for optimization of multiple responses. By keeping the minor contributing independent variable fixed at -1, 0, +1 the contours were constructed between the other independent variables for PS and drug entrapment efficiency separately. Two dimensional contour plots for PS and EE, were drawn between X_2 and X_3 at fixed value of X_1, from the reduced model equations (7), (8), (9) and (10). Fig. 4.4 A–C are the contour plots for TMD-NPs for prefixed PS values which were found to be curved segment representing non-linear relationship between variables X_2 and X_3. It was observed that minimum PS (<130nm) could be obtained with X2 between 50 mg and 60 mg and X_3 between 4.6 ml and 5 ml. Fig. 1D–F are the contour plots for PLGA NPs for prefixed PS values which were found to be curved segment representing non-linear relationship between variables X_2 and X_3. It was observed from Fig. 4.4D-F that that maximum EE (>72%) could be obtained with X_2 between 85 mg and 100 mg and entire range of X_3. Thus, the vertical curves signify that X3 contribute considerably lesser than X_2 for EE.

Overlay of contours is one of the technique for optimizing multiple responses. The overlay of PS and EE contour at 0 level of X1(overlay of 1B and 1D) is shown in Fig. 4.8. The desired criteria for unconjugated NPs are PS < 150 nm and EE > 70 %. It is observed from the Fig. that area formed by crossing of line for 72% EE and 140 nm PS, marked with arrow, is optimum. For optimization purpose, PS curves with size lesser than 150 nm were analysed for higher EE.

Fig. 4.6 A–C are the contour plots for LTG-NPs for prefixed PS values which were found to be curved segment representing non-linear relationship between variables X_2 and X_3. It was observed that minimum PS (<120nm) could be obtained with X2 between 40 mg and 50 mg and X_3 between 4.5 ml and 5 ml. Fig. 1D–F are the contour plots for PLGA NPs for prefixed PS values which were found to be curved segment representing non-linear relationship between variables X_2 and X_3. It was observed from Fig. 1D and 1F that that maximum EE (>72%) could be obtained with X_2 between 70 mg and 80 mg and entire range of X_3. Thus, the vertical curves signify that X_3 contribute considerably lesser than X_2 for EE.

The overlay of PS and EE contour at 0 level of X_1(overlay of 1B and 1D) is shown in Fig. 4.9. The desired criteria for unconjugated NPs are PS < 150 nm and EE > 70 %. It is observed from the Fig. that area between 130 and 140 nm PS contour curves crossed by 72% EE contour, marked with arrow, is optimum. For optimization purpose, PS curves with size

lesser than 150 nm were analysed for higher EE.

Check Point Analysis

For TMD, at fixed levels of -1, 0 and 1 of independent variable X_1, three check points were selected one each on three plotted contours. NPs at these three checkpoints were prepared experimentally using the same procedure keeping the other process variables as constant, with the amounts of X_2 and X_3 at the selected check points.

The computed values from the contours at -1, 0 and 1 level and the experimentally determined values for PS and drug entrapment efficiency values are shown in Table 4.10. Both experimentally obtained and theoretically computed PS and entrapment efficiency values were compared using student 't' test and the difference was found to be non significant ($p>0.05$).

Similarly for LTG, the check point batches were selected from contours plotted at fixed levels of -1, 0 and 1 of independent variable X_1 (for PS) and X_2 (for entrapment efficiency). The computed values from contours and the experimental values are recorded in Table 4.11 for PS and Table 4.12 for drug entrapment efficiency. Both experimentally obtained and theoretically computed PS and entrapment efficiency values were compared using student 't' test and the difference was found to be non significant ($p>0.05$).

Table 4.10: Check point analysis for TMD-NPs

X_1	Values From Contour Plots		PS (nm)		% EE	
	X_2	X_3	Calculated	Experimental*#	Calculated	Experimental*#
0.5	67.65	2.65	165.2	163.5 ± 5.4	68.32	67.12 ± 1.23
0.5	52.94	3.82	143.1	149.7 ± 4.6	59.25	58.34 ± 0.96
0.5	91.27	4.71	153.0	146.0 ± 2.3	71.71	69.88 ± 1.08
1	52.94	3.08	131.1	124.4 ± 3.8	55.50	55.10 ± 0.76
1	61.76	3.68	137.7	134.6 ± 4.5	61.16	63.25 ± 1.84
1	88.26	4.26	142.4	151.7 ± 6.1	68.95	69.53 ± 1.51
1.5	97.06	2.79	161.1	168.9 ± 3.5	72.57	71.22 ± 1.34
1.5	70.59	3.24	142.8	143.3 ± 4.2	62.72	63.34 ± 2.25
1.5	85.29	4.41	133.8	129.8 ± 5.2	63.92	62.67 ± 1.92

** Experimental values are represented as mean ± SD, n=3*

 # Difference from the calculated values not significant (p>0.05)

Table 4.11: Check point analysis for LTG-NPs

X_1	Values From Contour Plots		PS (nm)		% EE	
	X_2	X_3	Calculated	Experimental*#	Calculated	Experimental*#
0.5	44.71	2.79	140.3	136.4 ± 3.2	64.63	65.20 ± 2.12
0.5	72.94	3.24	154.1	146.6 ± 4.4	79.35	76.36 ± 1.40
0.5	51.76	4.85	127.9	121.4 ± 2.9	66.88	68.82 ± 1.94
1	77.65	2.65	160.2	165.8 ± 6.2	81.35	80.87 ± 1.75
1	61.18	3.09	138.2	137.5 ± 4.1	70.66	71.11 ± 0.97
1	42.35	4.56	113.9	110.2 ± 3.4	58.71	60.67 ± 2.24
1.5	47.06	2.65	129.2	135.9 ± 3.3	60.41	61.25 ± 1.35
1.5	63.53	3.38	133.2	141.2 ± 2.8	67.09	69.91 ± 1.57
1.5	75.29	4.26	129.6	135.6 ± 5.5	71.00	73.36 ± 1.68

** Experimental values are represented as mean ± SD, n=3*

 # Difference from the calculated values not significant (p>0.05)

This proves the role of a derived reduced polynomial equation and contour plots in the preparation of NPs of TMD and LTG of predetermined PS and drug entrapment efficiency within the selected range of the independent variables

Optimized batches

For TMD-NPs, the batch with PS of 141.1 ± 3.7 nm and drug entrapment efficiency of 73.57 ± 2.1 % prepared at 0 level of X_1 (1%w/v PVA in aqueous solution), +1 level of X_2 (100 mg polymer 5mg drug) and +1 level of X_3 (organic: aqueous phase of 1:2, i.e5 ml of organic phase and 10 ml of aqueous phase) was considered optimum based on the criteria of PS <150 nm with highest drug entrapment efficiency. Hence, 10 mg of drug and 100 mg of PLGA was dissolved in 5ml of acetone and this solution was added to 10 ml of 1%w/v PVA aqueous solution under constant moderate stirring.

Similarly for LTG-NPs, the batch with PS of 133.9 ± 3.6 nm and drug entrapment efficiency of 78.28 ± 1.7 % prepared at 0 level of X_1 (1%w/v PVA in aqueous solution), +1 level of X_2 (100 mg polymer 5mg drug) and +1 level of X_3 (organic: aqueous phase of 1:2, i.e 5 ml of organic phase and 10 ml of aqueous phase) was considered to be optimum.

Surface Response Plots

Response surface plots are very helpful in learning about both the main and interaction effects of the independent variables. These plots were plotted by keeping the factor X_1 at fixed levels (-1, 0 and 1). Response surface plots of TMD-NPs and LTG-NPs were shown in Fig 4.5 and 4.7 respectively.

Fig. 4.5A–C illustrates response surface plots for PS of TMD-NPs between X_2 and X_3, which shows an increase in PS with increase in the X_2 and decrease in X_3. Fig. 4.D–F illustrates response surface plots for EE of TMD-NPs between X2 and X_3, which depicts major positive effects of X2 on EE against minor decrease of EE with increase in X_3.

Similarly, Fig. 3A–C illustrates response surface plots for PS of LTG-NPs between X_2 and X_3, which shows an increase in PS with increase in the X_2 and decrease in X_3. Fig. 3D–F illustrates response surface plots for EE of LTG-NPs between X_2 and X_3, which depicts major positive effects of X_2 on EE against minor decrease of EE with increase in X_3.

4.3.2 Transferrin and Lactoferrin conjugation of Nanoparticles

The scheme of Tf/Lf conjugation to the NPs is shown in Fig. 4.2. The surface modification of NPs with Tf/Lf was achieved in two steps involving the activation of the NPs in the presence of catalyst zinc tetrafluoroborohydrate [$Zn(BF_4)_2$] with epoxy compound (SR-4GL, hexa epoxy) which acts as linker, followed by attachment of transferrin to the NPs at the other end of the epoxy compound. (Sahoo SK et al., 2004; Sahoo SK and Labhsetwar V, 2005). It is reported that PVA cross links with PLGA surface in the form of residual PVA. (Sahoo SK et al., 2002). As represented in the Fig. 4.6, atleast one of the epoxy of SR-4GL would have conjugated to the hydroxyl group of PVA and the other epoxy groups to the amine group of Tf/Lf. The amounts of activating agents SR-4GL and Tf/Lf were optimized to achieve minimum increase in PS and maximum Tf/Lf density on the surface of NPs.

The amount of the catalyst was kept at 10 mg during the entire conjugation study. The influence of the amount of epoxy compound on the density of surface Tf/Lf and PS was evaluated keeping the amount of NPs and the amount of Tf/Lf constant at 75 mg and 1 mg respectively and the results recorded in Table 4.12 and 4.13 and graphically shown in Fig. 4.10. The influence of the amount ligand on the density of surface Tf/Lf and PS was evaluated keeping the amount of NPs and the amount of SR-4GL constant at 75 mg and 10 mg respectively and the results recorded in Table 4.14 and 4.15 and graphically shown in Fig. 4.11.

Table 4.12: Influence of the concentration of the activating agent SR-4GL on Tf/Lf density and PS of TMD-NPs

SR-4GL (mg)	Tf-TMD-NPs			Lf-TMD-NPs		
	Tf density (µg/mg)	Conju. Efficiency (%)	PS (nm)	Lf density (µg/mg)	Conju. Efficiency (%)	PS (nm)
5	6.3 ± 0.3	47.3 ± 2.0	151.3 ± 5.0	6.5 ± 0.2	48.8 ± 1.5	150.9 ± 4.1
10	**10.6 ± 0.2**	**79.5 ± 1.9**	**157.5 ± 4.2**	**11.1 ± 0.2**	**83.3 ± 1.8**	**158.8 ± 3.9**
20	11.1 ± 0.3	83.3 ± 2.2	175.1 ± 3.9	11.4 ± 0.3	85.5 ± 2.1	173.4 ± 4.5

Values are represented as mean ± SD, n=3

Table 4.13: Influence of the Tf/Lf concentration on Tf/Lf density and PS of TMD-NPs

Tf/Lf (mg)	Tf-TMD-NPs			Lf-TMD-NPs		
	Tf density (µg/mg)	Conju. Efficiency (%)	PS (nm)	Lf density (µg/mg)	Conju. Efficiency (%)	PS (nm)
0.25	3.2 ± 0.1	96.0 ± 1.8	149.2 ± 3.9	3.3 ± 0.1	97.5 ± 2.2	152.6 ± 2.8
0.5	5.9 ± 0.2	88.5 ± 2.3	152.9 ± 4.3	6.0 ± 0.1	90.0 ± 1.3	156.4 ± 4.2
1.0	**10.6 ± 0.2**	**79.5 ± 1.9**	**157.5 ± 4.2**	**11.1 ± 0.2**	**83.3 ± 1.8**	**158.8 ± 3.9**
1.5	13.1 ± 0.3	65.5 ± 1.5	168.9 ± 5.8	13.5 ± 0.3	67.5 ± 1.4	171.9 ± 5.0

Values are represented as mean ± SD, n=3

Table 4.14: Influence of the concentration of the activating agent SR-4GL on Tf/Lf density and PS of LTG-NPs

SR-4GL (mg)	Tf-TMD-NPs			Lf-TMD-NPs		
	Tf density (µg/mg)	Conju. Efficiency (%)	PS (nm)	Lf density (µg/mg)	Conju. Efficiency (%)	PS (nm)
5	6.7 ± 0.1	50.3 ± 0.9	146.9 ± 4.0	6.9 ± 0.2	51.8 ± 1.2	144.2 ± 5.1
10	**10.7 ± 0.2**	**80.3 ± 1.5**	**151.0 ± 3.8**	**11.4 ± 0.1**	**85.5 ± 0.9**	**150.4 ± 4.0**
20	11.3 ± 0.2	84.8 ± 1.4	168.7 ± 5.9	11.9 ± 0.3	89.3 ± 2.2	166.5 ± 3.3

Values are represented as mean ± SD, n=3

Table 4.15: Influence of the Tf/Lf concentration on Tf/Lf density and PS of LTG-NPs

Tf/Lf (mg)	Tf-TMD-NPs			Lf-TMD-NPs		
	Tf density (µg/mg)	Conju. Efficiency (%)	PS (nm)	Lf density (µg/mg)	Conju. Efficiency (%)	PS (nm)
0.25	3.3 ± 0.1	98.4 ± 2.4	140.2 ± 3.0	3.3 ± 0.1	97.8 ± 1.9	142.5 ± 2.8
0.5	6.0 ± 0.1	90.0 ± 1.4	144.9 ± 4.6	6.1 ± 0.2	91.7 ± 2.3	147.3 ± 4.2
1.0	**10.7 ± 0.2**	**80.3 ± 1.5**	**151.0 ± 3.8**	**11.4 ± 0.1**	**85.5 ± 0.9**	**150.4 ± 4.0**
1.5	13.0 ± 0.2	65.0 ± 1.1	163.5 ± 3.2	13.8 ± 0.4	69.0 ± 1.6	161.9 ± 5.0

Values are represented as mean ± SD, n=3

Tramadol Nanoparticles

Influence of amount of activating agent [Epoxy compound: SR-4GL]

The amount of epoxy compound was varied at 5 mg, 10 mg and 20 mg. With the increase in the amount of the epoxy from 5 to 10 mg, the surface Tf density for Tf-TMD-NPS increased from 6.3 µg/mg to 10.6 µg/mg and the PS increased from 151.3 nm to 157.5 nm. Increasing further the epoxy compound to 20 mg did not considerably increase the surface Tf density. However, the PS increased from 157.5 nm to 175.1 nm. Similar results were observed for Lf conjugation. The epoxy compound amount at 5, 10 and 20 mg resulted in the surface Lf density of 6.5 µg/mg, 11.4 µg/mg and 11.4 µg/mg respectively, with corresponding PS of 150.9 nm, 158.8 nm and 173.4 nm. Conjugation efficiency of Tf and Lf to TMD-NPs at 10 mg SR-4GL, were 79.5 and 83.3 respectively. The increase in the surface Tf/Lf density may be due to the increase in the number of the epoxy molecules reacting with hydroxyl of PVA and thereby increase in the availability of the epoxy groups for conjugation of Tf/Lf. The association of epoxy and ligand with NPs is believed to have resulted in the increase in the PS. Increasing the epoxy amount from 10 mg to 20 mg resulted in much increase in the PS but the amount of the ligand conjugated did not increase significantly. Hence, the epoxy amount was optimized at 10 mg for both Tf and Lf conjugation with TMD-NPs.

Figure 4.10: Influence of the concentration of the activating agent SR-4GL on Tf/Lf density and PS of TMD-NPs (A) Tf-TMD-NPs (B) Lf-TMD-NPs

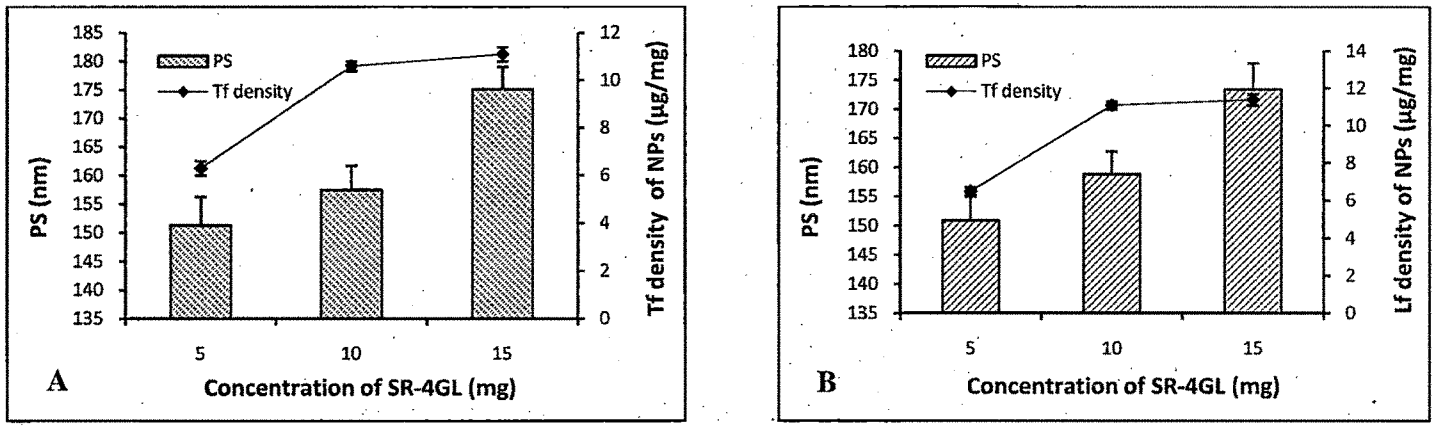

Figure 4.11: Influence of the Tf/Lf concentration on Tf/Lf density and PS of TMD-NPs (A) Tf-TMD-NPs (B) Lf-TMD-NPs

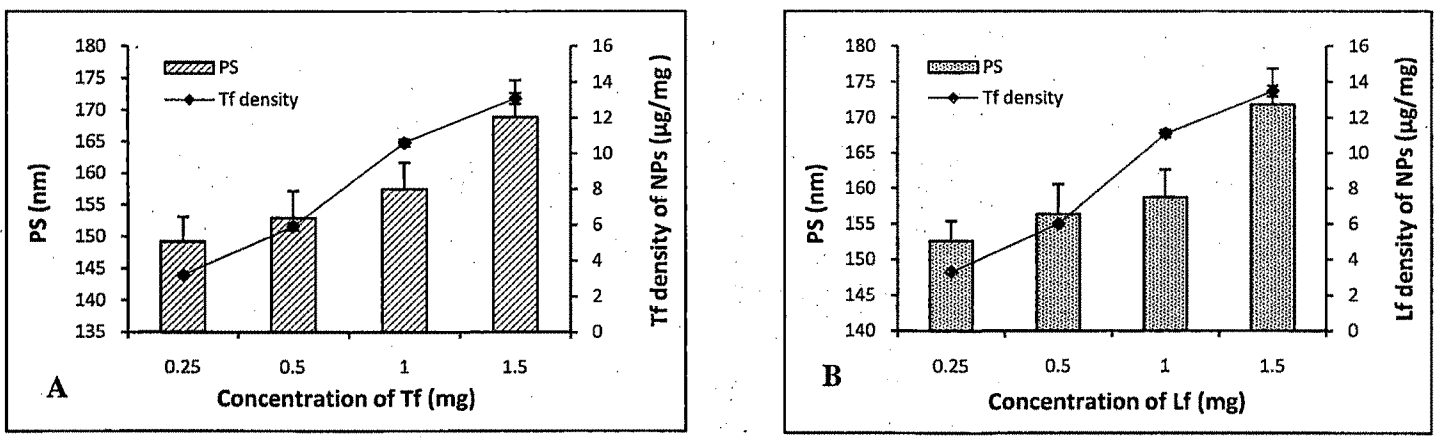

Figure 4.12: Influence of the concentration of the activating agent SR-4GL on Tf/Lf density and PS of LTG-NPs (A) Tf-LTG-NPs (B) Lf-LTG-NPs

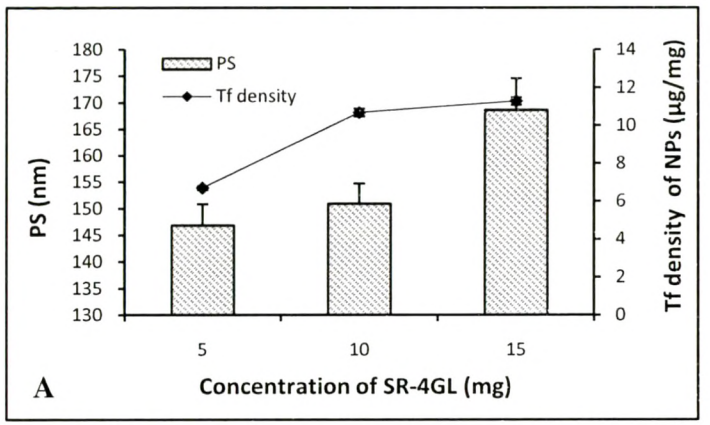

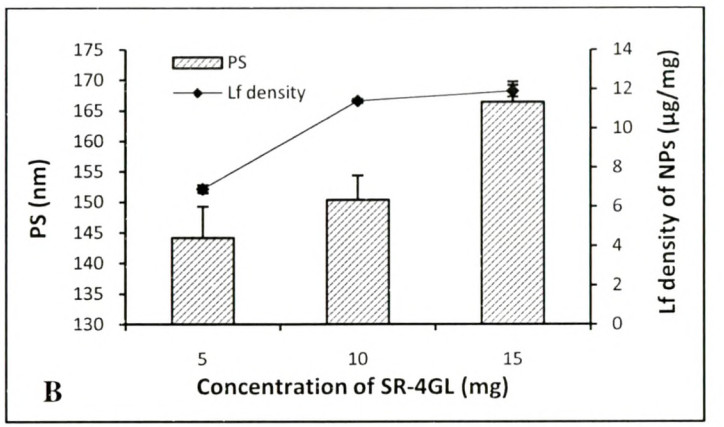

Figure 4.13: Influence of the Tf/Lf concentration on Tf/Lf density and PS of LTG-NPs (A) Tf-LTG-NPs (B) Lf-LTG-NPs

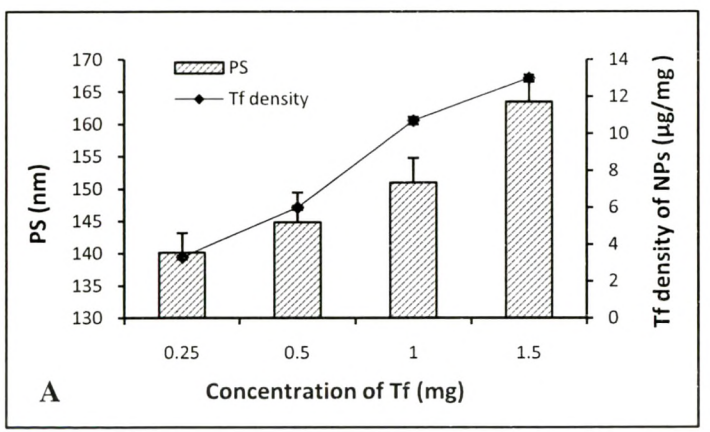

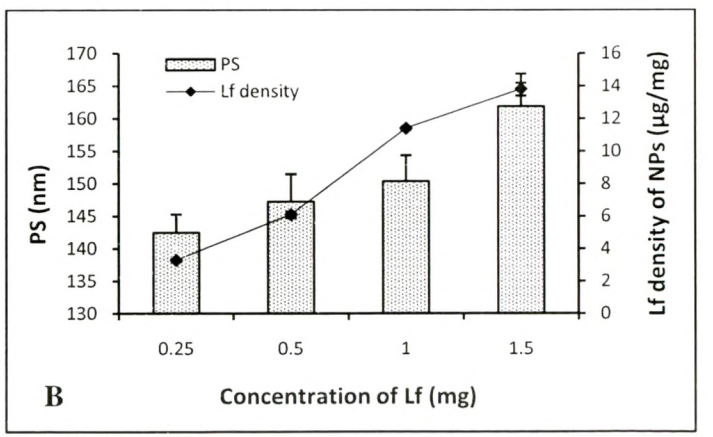

Influence of the ligand concentration

The amount of Tf was varied from 0.25 mg to 1.5 mg. For TMD-NPs, with increase in the amount of Tf from 0.25 mg to 1.0 mg, the surface Tf density increased from 3.2 µg/mg to 10.6 µg/mg and the PS increased from 149.2 nm to 157.5 nm. Further increasing the amount of Tf from 1.0 mg to 1.5 mg, the Tf density increased from 10.6 µg/mg to 13.1 µg/mg. But the PS increased from 157.5 to 168.9 nm. Also, the conjugation efficiency dropped from 79.6 to 65.5 with increase in Tf from 1.0 to 1.5 mg. Similarly, for Lf conjugation surface Lf density and PS were found to increase from 3.3 µg/mg to 13.5 µg/mg and 152.6 nm to 171.9 nm respectively when Lf amount was varied from 0.25mg to 1.5 mg.

With increase in the amount of Tf/Lf added for conjugation, the increase in the surface Tf/Lf density could have been due to the increase in the Tf molecule density available for conjugation. The increase in the PS could have been due to increased surface Tf/Lf density. At the highest amount of Tf added for conjugation i.e 1.5 mg, the PS increased, probably due to the cross linking of Tf/Lf molecule with the epoxy groups of the neighboring molecules. Also. Conjugation efficiency were around 65-67 % at 1.5 mg ligand compared to 80-83 % at 1.0. For, intravenous administration, the preferable PS is below 200nm and hence considering the size and conjugation efficiency, 1.0 mg of Tf/Lf was considered as optimized amount.

Lamotrigine Nanoparticles

Influence of amount of activating agent [Epoxy compound: SR-4GL]

The amount of epoxy compound was varied at 5 mg, 10 mg and 20 mg. With the increase in the amount of the epoxy from 5 to 10 mg, the surface Tf density for Tf-LTG-NPs increased from 6.7 µg/mg to 10.7 µg/mg and the PS increased from 146.9 nm to 151.0 nm. Increasing further the epoxy compound to 20 mg did not considerably increase the surface Tf density. However, the PS increased from 151.0 nm to 168.7 nm. Similar results were observed for Lf conjugation. The epoxy compound amount at 5, 10 and 20 mg resulted in the surface Lf density of 6.9 µg/mg, 11.4 µg/mg and 11.9 µg/mg respectively, with corresponding PS of 144.2 nm, 150.4 nm and 166.5 nm. Conjugation efficiency of Tf and Lf to LTG-NPs at 10 mg concentration of SR-4GL, were 80.3 and 85.5 respectively.

The increase in the surface Tf/Lf density may be due to the increase in the number of the epoxy molecules reacting with hydroxyl of PVA and thereby increase in the availability of the epoxy groups for conjugation of Tf/Lf. The association of epoxy and ligand with NPs is

believed to have resulted in the increase in the PS. Increasing the epoxy amount from 10 mg to 20 mg resulted in much increase in the PS but the amount of the ligand conjugated did not increase significantly. Hence, the epoxy amount was optimized at 10 mg for both Tf and Lf conjugation with LTG-NPs.

Influence of the ligand concentration

The amount of Tf was varied from 0.25 mg to 1.5 mg. For LTG-NPs, with increase in the amount of Tf from 0.25 mg to 1.0 mg, the surface Tf density increased from 3.3 µg/mg to 10.7 µg/mg and the PS increased from 140.2 nm to 151.0 nm. Further increasing the amount of Tf from 1.0 mg to 1.5 mg, the Lf density increased from 10.7 µg/mg to 13.0 µg/mg. But the PS increased from 151.0 nm to 163.5 nm. Also. the conjugation efficiency dropped from 80.3 to 65.0 with increase in Tf from 1.0 to 1.5 mg.

Similarly, for Lf conjugation surface Lf density and PS were found to increase from 3.3 µg/mg to 13.8 µg/mg and 142.5 nm to 161.9 nm respectively when Lf amount was varied from 0.25mg to 1.5 mg. With increase in the amount of Tf/Lf added for conjugation, the increase in the surface Tf/Lf density could have been due to the increase in the Tf molecule density available for conjugation. The increase in the PS could have been due to increased surface Tf/Lf density. At the highest amount of Tf added for conjugation i.e 1.5 mg, the PS increased, probably due to the cross linking of Tf/Lf molecule with the epoxy groups of the neighboring molecules. Also. Conjugation efficiency was around 65-69 % at 1.5 mg ligand compared to 80-85 % at 1.0. For, intravenous administration, the preferable PS is below 200nm and hence considering the size and conjugation efficiency, 1.0 mg of Tf/Lf was considered as optimized amount.

The conjugation amino of Tf and Lf with the methylene of epoxy compound was confirmed by ^{1}H-NMR. Fig. 4.14 and 4.15 represent the ^{1}H-NMR of TMD-NPs and LTG-NPs. For TMD-NPs and LTG-NPs the peaks at around 2.2 to 2.3 ppm were observed representing the conjugation of amino group of Tf and Lf to the methylene group of epoxy compound.

Figure 4.14: ^{1}H-NMR of (A) Tf -TMD-NPs and (B) Lf-TMD-NPs

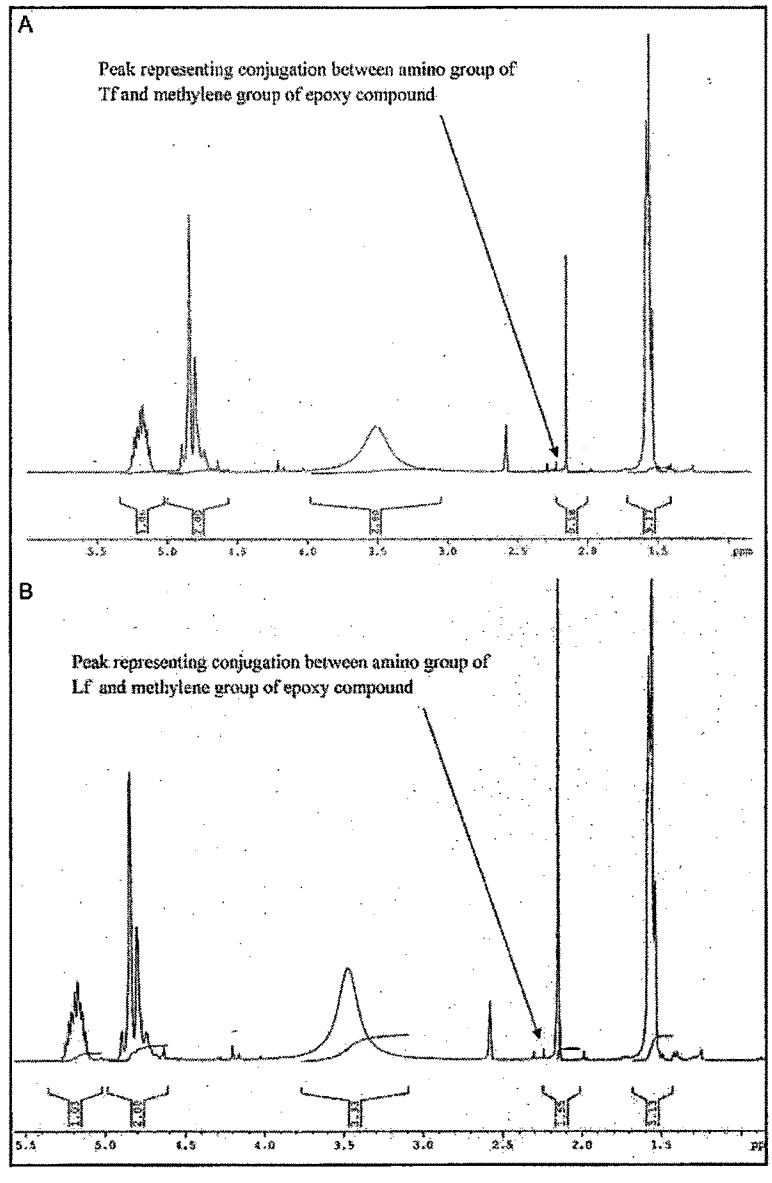

Figure 4.15: ^{1}H-NMR of (A) Tf -LTG-NPs and (B) Lf-LTG-NPs

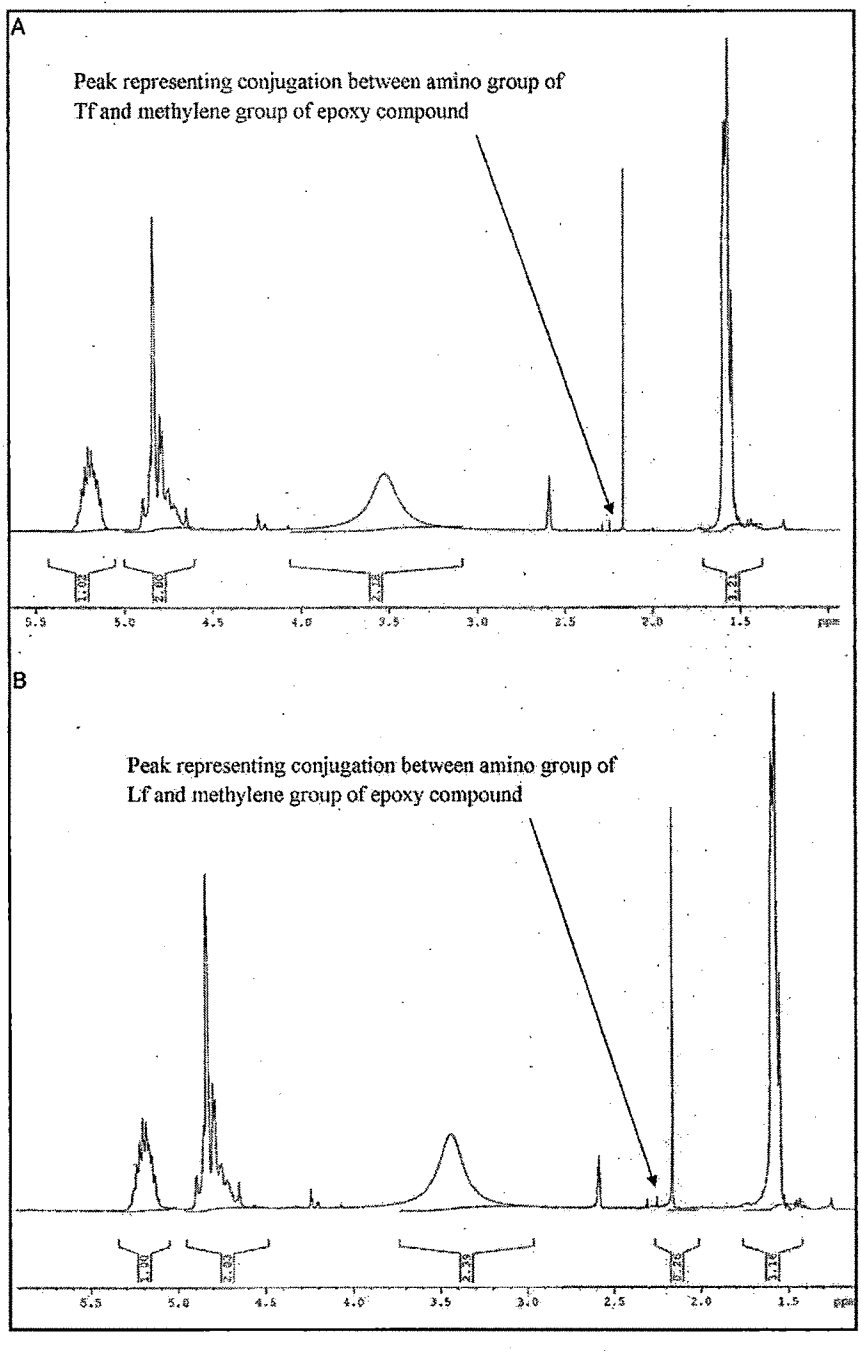

4.3.3 Lyophilization and optimization of lyoprotectant concentration

Freeze-drying has been the most utilized drying method of NPs suspensions. Because the freeze-drying process is highly stressful for NPs, addition of lyoprotectants becomes essential. For NPs carbohydrates have been perceived to be suitable freeze-drying protectants. There are considerable differences in the lyoprotective abilities of different carbohydrates.

The optimized batch of NPs was lyophilized using sucrose, mannitol and trehalose (at 1:1, 1:2 and 1:3 NPs: lyoprotectant) to select suitable lyoprotectant and its concentration and recorded in Table 4.16. The redispersibility of the freeze-dried formulations and PS of the NPs before and after freeze-drying were evaluated and recorded in Table 4.17.

Table 4.16: Effect of different lyoprotectants and its concentration on the PS and redispersibility of TMD-NPs

Lyoprotectant	NP:Lyoprotectant	Aggregation	Redispersibility	Tyndall effect	Sf/Si
Nil	-	+++	Absent	-	ND
Sucrose	1:1	++	Absent	-	ND
	1:1.5	+	Poor	-	3.48
	1:2	+	Poor	-	2.74
Mannitol	1:1	+	Poor	-	3.72
	1:1.5	+	Poor	-	3.07
	1:2	+	Poor	-	2.49
Trehalose	1:1	-	Easy	+	2.25
	1:1.5	-	Easy	++	1.52
	1:2	-	Easy	+++	1.01

Values of size represented as mean ± SD, n=3

ND: Not Determined, Si=Initial size, Sf= final size

Table 4.17: Effect of Trehalose on the PS and redispersibility of NPs formulations

Formulation	NP:Lyoprotectant	Aggregation	Redispersibility	Tyndall effect	Sf/Si
TMD-NPs	1:2	-	Easy	+++	1.01
Tf-TMD-NPs	1:2.25	-	Easy	++	1.02
Tf-TMD-NPs	1:2.25	-	Easy	++	1.02
LTG-NPs	1:2	-	Easy	+++	1.00
Lf-LTG-NPs	1.2.25	-	Easy	++	1.01
Tf-LTG-NPs	1:2.25	-	Easy	++	1.02

Values of size represented as mean ± SD, n=3

Si=Initial size, Sf= final size

Figure 4.16: Effect of different lyoprotectants and its concentration on the PS and redispersibility of TMD-NPs

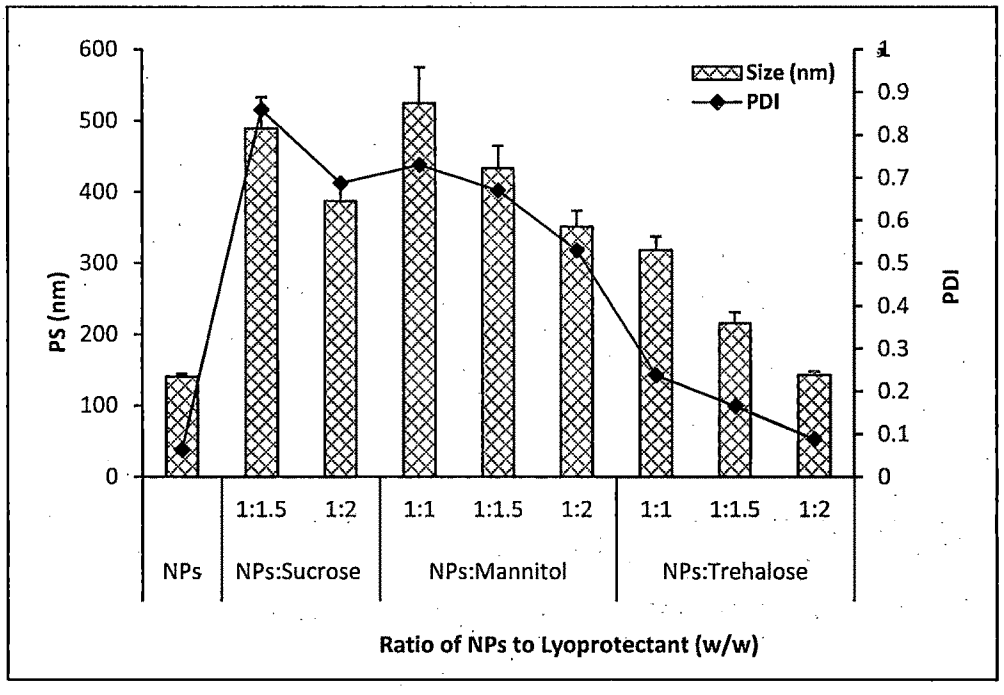

Effect of different lyoprotectants and its concentration on the PS and redispersibility and aggragation behavior of TMD-NPs was shown in Table 4.16.

With use of sucrose as the lyoprotectant, the cake formed after lyophilization was condensed and had collapsed structure. At lowest ratio of 1:1, the lyophilized NPs could not be redispersed. For the ratios of 1:15 and 1:2 PS of the NPs, as shown in Table 4.13, increased significantly after lyophilization. The S_f/S_i values were 3.48, 2.74 with 1:1.5, 1:2 NPs: sucrose respectively. Redispersibility was achieved only after sonication. The increase in the PS could have been due to the cohesive nature of the sucrose. Further, it was observed that the lyophilized NPs with sucrose had tendency to absorb moisture very quickly.

In the presence of mannitol, the visual inspection of the lyophilised products reveal that the cakes formed were voluminous, fluffy and did not show any signs of shrinkage after the freeze drying process. However, redispersion of mannitol was difficult and possible only after vigorous shaking. Possibly, the polyalcohol structure tends to form of a crystalline mass during lyophilisation process. (Franks F, 1998). PS data with mannitol reveals a significant increase in PS after lyophilisation. The S_f/S_i values were 2.98, 2.49 and 2.25 with 1:1, 1:1.5 and 1:2 NPs: mannitol respectively.

With trehalose, all the lyophilized cakes were snow-like, voluminous and easy to reconstitute (Sameti M et al, 2003). The increase in PS was not significant as indicated by S_f/S_i values which were 2.52, 1.52, and 1.01 for 1:1, 1:1.5 and 1:2 NPs: trehalose respectively recorded in Table 5. Also the tyndall effect observed with NPs was retained after redispersion of the NPs lyophilized using trehalose. Therefore, trehalose at a ratio of 1:2 (NPs: trehalose) was used as lyoprotectant for lyophilization of optimized batch of NPs. Also, it was found satisfactory for LTG-NPs without any significant change observed against initial. Further it was found satisfactory at 1:2.25 ratios for conjugated NPs of TMD. The superior lyoprotective effect may be attributed to the ability of trehalose to form a glassy amorphous matrix around the particles, through hydrogen-bonding with polar groups of the product, preventing the particles from sticking together during removal of water (Konan YR et al., 2002). Trehalose was found effective lyoprotectant for variety of pharmaceutical and biological materials (De Jaeghere F et al, 1999). Therefore, trehalose at a ratio of 1:2.5 (NPs: trehalose) was used as lyoprotectant for lyophilization of optimized batch of NPs for further studies.

For further studies, TMD NPs were prepared using 10 mg drug, 100 mg PLGA, 10 ml of 1%w/v PVA concentration in aqueous phase and organic: aqueous phase ratio of 0.5 (5ml of organic phase for 10ml of aqueous phase). For LTG NPs were prepared in similar manner using 80 mg of PLGA. The optimized NPs were conjugated with transferrin using 10 mg epoxy activating agent and 1 mg transferrin for 75 mg of NPs. .The NPs were lyophilized using trehalose as cryoprotectant at 1:3 (NPs: trehalose) ratio. The unconjugated and conjugated NPs of TMD and LTG were characterized and subjected to stability studies.

4.3.4 Characterization of Nanoparticles

Table 4.18: PS, PDI, ZP, %EE, %Residual PVA of unconjugated & conjugated NPs

Formulations	Evaluation parameters				
	PS (nm)	PDI	ZP (mV)	%EE	% Residual PVA
TMD-NPs	141.1 ± 3.7	0.053	-10.32 ± 0.48	73.57 ± 2.1	5.8 ± 0.4
Tf-TMD-NPs	157.5 ± 4.2	0.091	-11.06 ± 0.41	71.49 ± 1.6	-
Lf-TMD-NPs	158.8 ± 3.9	0.111	-9.35 ± 0.29	71.16 ± 2.8	-
LTG-NPs	133.9 ± 3.6	0.048	-12.07 ± 0.33	78.28 ± 1.7	5.6 ± 0.3
Tf-LTG-NPs	151.0 ± 3.8	0.107	-12.88 ± 0.46	76.05 ± 1.8	-
Lf-LTG-NPs	150.4 ± 4.0	0.083	-11.21 ± 0.35	76.74 ± 1.3	-

Each value is represented as mean ± SD, n=3

Figure 4.17: TEM images of (A) TMD-NPs, (B) Lf-TMD-NPs and (C) Tf-TMD-NPs.

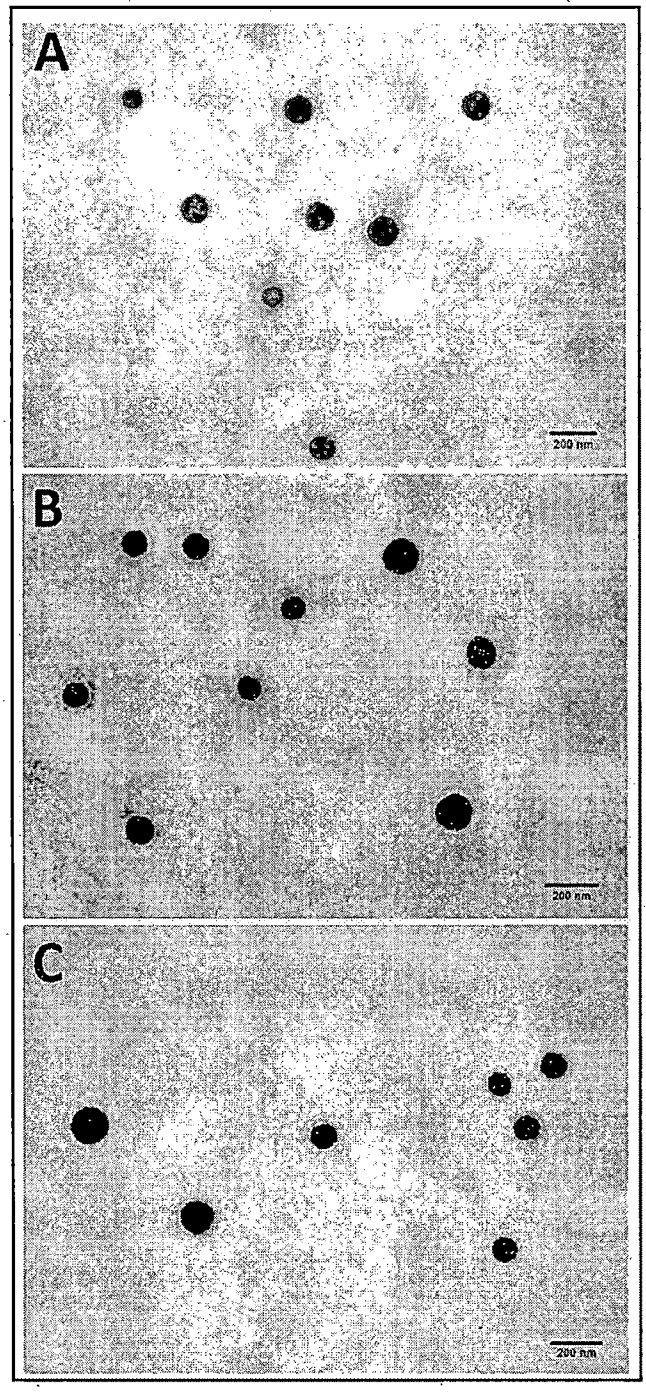

Figure 4.18: TEM images of (A) LTG-NPs, (B) Lf-LTG-NPs and (C) Tf-LTG-NPs.

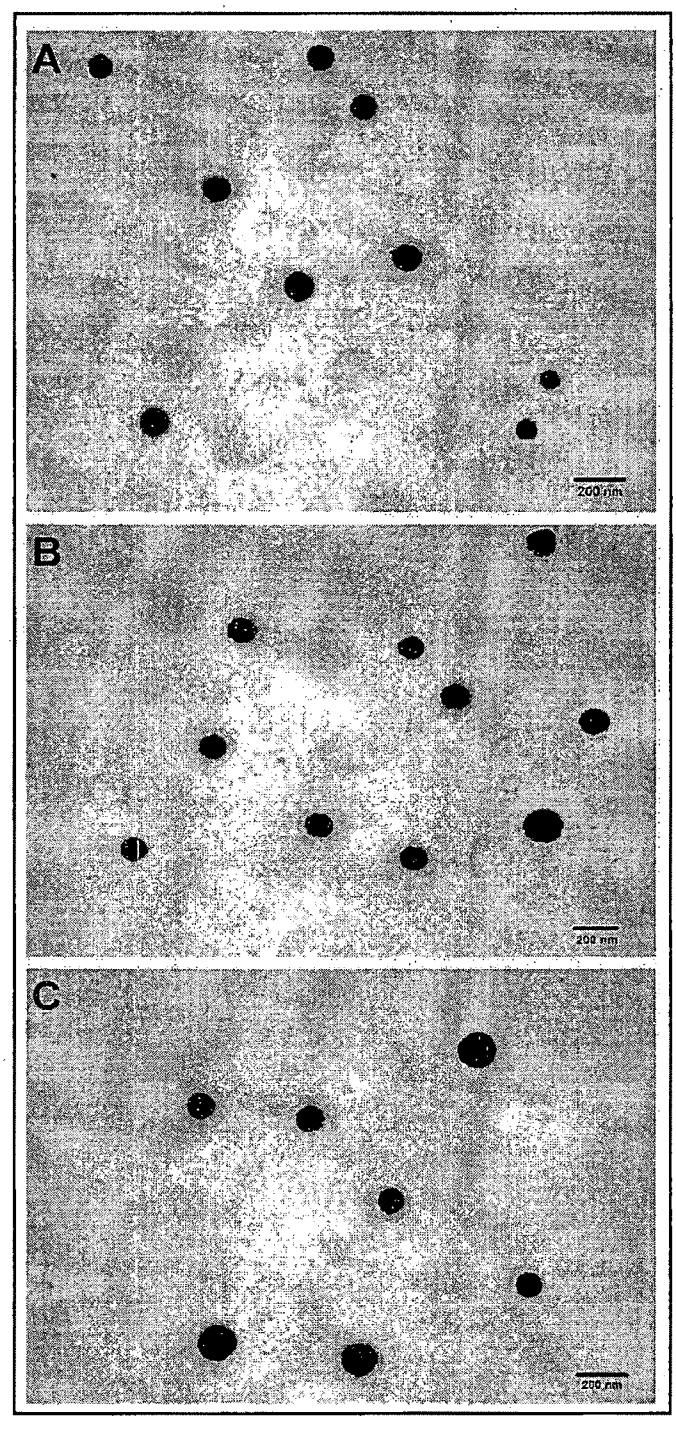

Figure 4.19: DSC thermogram of (A) TMD-NPs (B) TMD (C) PLGA and (D) PVA.

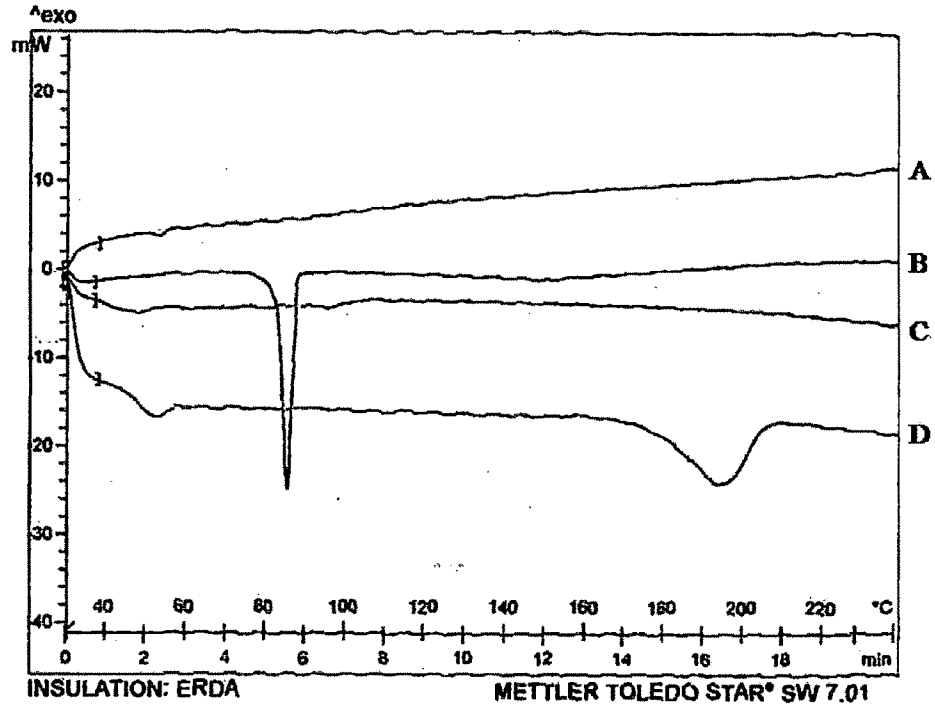

Figure 4.20: DSC thermogram of (A) LTG-NPs (B) LTG (C) PLGA and (D) PVA

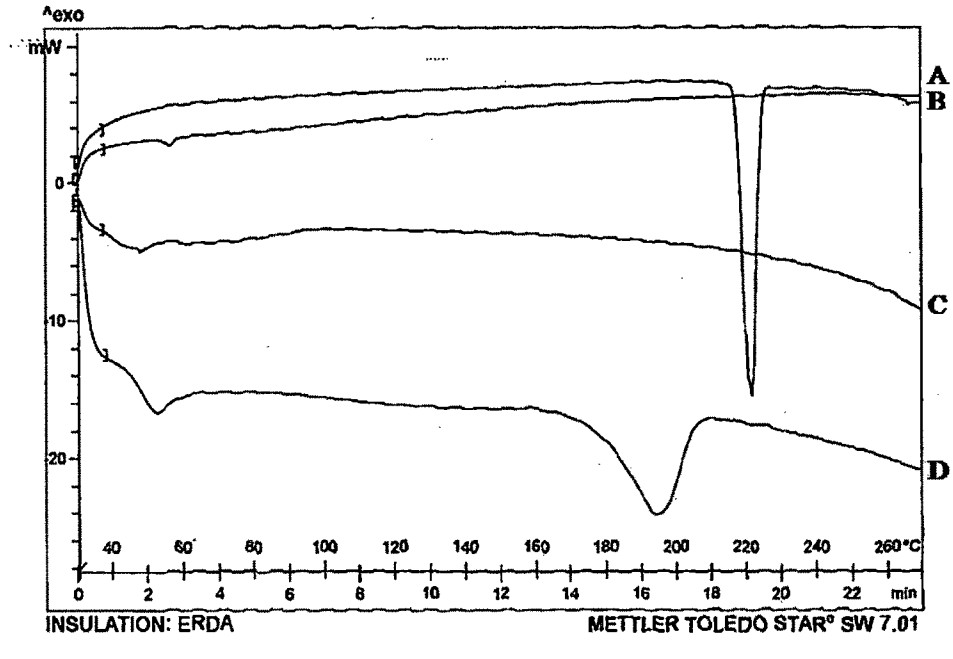

Figure 4.21: *In vitro* release profile of TMD from conjugated and unconjugated NPs

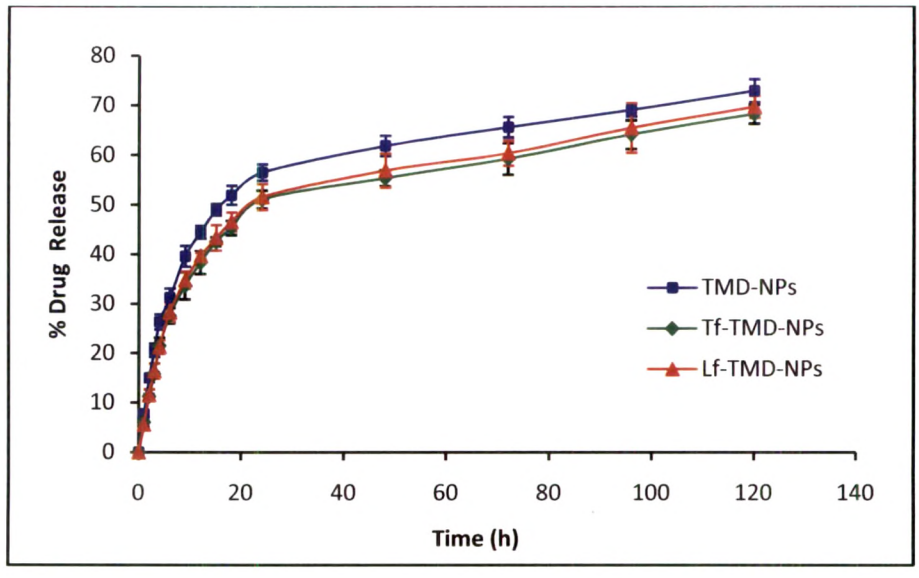

Figure 4.22: *In vitro* release profile of LTG from conjugated and unconjugated NPs

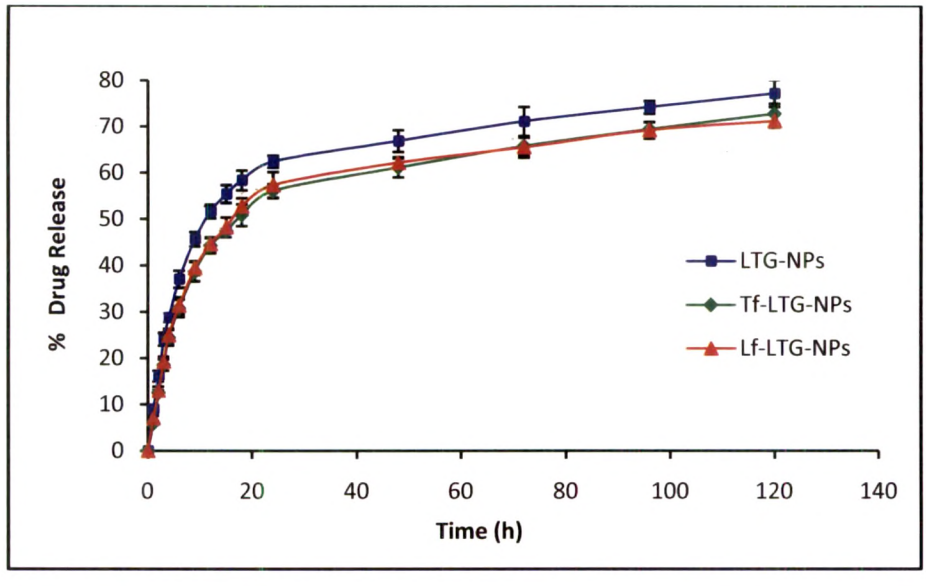

Table 4.19: Mathematical modeling of release profile of TMD from NPs

Formulation	Model	R^2 value	Equation
TMD-NPs	Zero order	0.670	y = 0.444x + 30.04
	First order	0.809	y = -0.004x + 1.842
	Higuchi	0.639	y = 8.406x
	Hixson Crowell	0.617	y = -0.012x + 1.611
	Korsmeyer peppas	**0.884**	y = 0.417x - 0.893
Tf-TMD-NPs	Zero order	0.708	y = 0.437x + 25.14
	First order	0.828	y = -0.003x + 1.873
	Higuchi	0.752	y = 7.587x
	Hixson Crowell	0.549	y = -0.013x + 1.794
	Korsmeyer peppas	**0.895**	y = 0.460x - 1.008
Lf-TMD-NPs	Zero order	0.704	y = 0.447x + 25.63
	First order	0.831	y = -0.003x + 1.870
	Higuchi	0.752	y = 7.749x
	Hixson Crowell	0.54	y = -0.013x + 1.781
	Korsmeyer peppas	**0.885**	y = 0.470x - 1.013

Table 4.20: Mathematical modeling of release profile of LTG from NPs

Formulation	Model	R^2 value	Equation
TMD-NPs	Zero order	0.619	y = 0.453x + 34.53
	First order	0.780	y = -0.004x + 1.809
	Higuchi	0.524	y = 9.180x
	Hixson Crowell	0.484	y = -0.012x + 1.472
	Korsmeyer peppas	**0.862**	y = 0.402x - 0.827
Tf-TMD-NPs	Zero order	0.672	y = 0.460x + 28.61
	First order	0.813	y = -0.004x + 1.851
	Higuchi	0.696	y = 8.334x
	Hixson Crowell	0.511	y = -0.013x + 1.679
	Korsmeyer peppas	**0.866**	y = 0.462x - 0.966
Lf-TMD-NPs	Zero order	0.645	y = 0.445x + 29.61
	First order	0.777	y = -0.003x + 1.842
	Higuchi	0.644	y = 8.36x
	Hixson Crowell	0.502	y = -0.012x + 1.641
	Korsmeyer peppas	**0.873**	y = 0.441x - 0.931

The PS, PDI, ZP, %EE and residual PVA for TMD and LTG NPs are recorded in Table 4.18. The PS of unconjugated NPs was found in the range of 141.1-158.8 nm. Lower PS (< 200 nm) (Modhimi SM et al., 1993) suggests suitability of formulation for intravenous applications. Poly dispersity index (PDI) observed to be < 0.1 suggest uniform PS distribution. There was a minor increase in size of NPs due to conjugation as reflected from PS of Tf and Lf conjugated NPs. ZP of NPs were found in the range of -12.88 to -9.35 mV. ZP of NPs was negative due to the presence of terminal carboxylic groups in the polymers. Negative ZP imparts stability against particle-particle agglomeration. A marginal decrease was observed in ZP with Tf however, the ZP increases after conjugation with Lf due to its electro positive nature. The drug encapsulation efficiency for all NPs formulation was found to be higher than 70% indicating good efficiency of the nanoprecipation method for selected drugs. The residual PVA associated with the NPs surface was 5.8 ± 0.4% & 5.6 ± 0.3% w/w of NPs for unconjugated TMD and LTG NPs respectively.

TEM study (Fig. 4.17 & 4.18) revealed that the unconjugated and surface modified NPs were almost spherical in shape without agglomeration. The size observed by TEM was in accordance with PCS measurement.

DSC study (Fig. 4.19 & 4.20) was performed to investigate the physical state of the drug in the NPs. PLGA shows a Tg rather than Tm (melting point), indicating the presence of the polymer in amorphous form. TMD had an endothermic peak of melting at 84-86°C whereas drug-loaded NPs had no such peak indicating molecularly dispersed drug in polymer matrix. Similarly LTG has endothermic peak at 217-220-°C, drug-loaded NPs had no such peak indicating molecularly dispersed drug in polymer matrix.

In vitro drug release from TMD and LTG loaded NPs (conjugated and unconjugated) upto 5 days summarized as cumulative percentage release was shown in Fig 4.21 and 4.22 respectively. An initial burst release of approximately 20% was observed within 4 h, which may be attributed to the presence of TMD or LTG present at the surface of the NPs. More than 50 % of drug was released within one day for all NP formulations. After this phase, prolonged release was observed up to 5 days, showing a typical sustained drug release indicative of drug diffusion and matrix erosion mechanisms (Holland SJ and Tighe BJ, 1992).

The mathematical modeling of release data was performed by fitting % drug release in given time in different order kinetics like zero order, first order, Higuchi, Hixon Crowell, and Korsmeyer peppas. Regression coefficients of all formulations in different orders were

compared and it was found that the release pattern of TMD and LTG from the formulation follow Korsmeyer peppas model.

The release of the drug from PLGA is by the degradation of polymer which occurs by hydrolysis of its ester linkages in presence of water. The general mechanism by which an active agent is released from a delivery vehicle is a combination of diffusion of an active agent from the polymer matrices, bulk erosion of the polymer, swelling and degradation of the polymer. The degradation of PLGA is slow, therefore the release of TMD and LTG from NPs may depend on drug diffusion and PLGA surface and bulk erosion or swelling (Mu and Feng 2003).

4.4 Conclusion

PLGA NPs of TMD and LTG were successfully prepared by nanoprecipitation method. The NPs were surface conjugated with transferrin for preferential brain delivery. The particle observed for both unconjugated and conjugated NPs of TMD and LTG have small PS (<200nm) suitable for intravenous administration. The smooth and spherical surface of NPs was confirmed from TEM. The DSC studies indicate the presence of the drug in NPs as molecularly dispersed form. A prolonged release was observed up to 120 hrs for both unconjugated and conjugated NPs of both drugs. The NPs were further subjected to stability studies according to ICH guidelines (Chapter 6).

4.5 References

- Akhnazarova S, Kafarov V. 1982. Experiment Optimization in Chemistry and Chemical Engineering, Mir publications, Moscow.
- Bilati U, Allémann E, Doelker E. 2005. "Development of a nanoprecipitation method intended for the entrapment of hydrophilic drugs into NPs." *Eur J Pharm Sci* 24(1): 67-75.
- Box GEP, Wilson KB. 1951. On the experimental attainment of optimum conditions. 9th ed. Amsterdam: *J Roy Stat Soc* 113: 1-45.
- Budhian A, Siegel SJ, Winey KI. 2005. Production of haloperidol-loaded PLGA NPs for extended controlled drug release of haloperidol. J *Microencapsulation* 22:773–785.
- Byrnea JD, Betancourtb T, Peppas BL. 2008. Active targeting schemes for NPs systems in cancer therapeutics. *Adv Drug Deliv Rev* 60(15): 1615-1626.
- Chorny M., Fishbein I, Danenberg HD , Golomb GL. 2002. Lipophilic drug loaded nanospheres prepared by nanoprecipitation: effect of formulation variables on size, drug recovery and release kinetics. *Journal of Control Release* 83 : 389–400.
- De Jaeghere F, Alle´ mann E, Leroux JC, Stevels W, Feijen J, Doelker E, Gurny R. 1999. Formulation and lyoprotection of poly (lactic acid-co-ethylene oxide) NPs: influence on physical stability and in vitro cell uptake. *Pharm Res* 16: 859–866.
- Derakhshandeh K, Erfan M, Dadashzadeh S. 2007. Encapsulation of 9-nitrocamptothecin, a novel anticancer drug, in biodegradable NPs: Factorial design, characterization and release kinetics. *Eur J Pharm Biopharm* 66 :34–41.
- Derringer G, Suich R. 1980. Simultaneous optimization of several response variables. *J Quality Technology*12: 214–218.
- Feng SS. 2004. Nanoparticles of biodegradable polymers for new-concept chemotherapy. *Expert Reviews Medical Devices* 1 (1): 115-125.
- Fessi H, Puisieux F, Devissaguet JP, Ammoury N and Benita S. 1989. Nanocapsule formation by interfacial polymer deposition following solvent displacement. *Int J Pharm* 55:R1-R4.
- Franks F, 1998. Freeze-drying of bioproducts: putting principles into practise. *Eur J Pharm Biopharm* 45: 221–229.
- Galindo-Rodriguez S, Allemann E, Fessi H, Doelker E. 2004. Physicochemical parameters associated with NPs formation in the salting-out, emulsification-diffusion and nanoprecipitation methods. *Pharm Res* 21: 1428–1439.

- Holland SJ, Tighe BJ. 1992. Biodegradable polymers. In: Garderton, D, Jones T ed. Advanced Pharmaceutical Sciences, vol. 6. New York: Academic Press, 101–164.
- Huang B, Tsai YH, Lee SH, Chang JS, Wu PC. 2005. Optimization of pH independent release of nicardipine hydrochloride extended-release matrix tablets using response surface methodology. *Int J Pharm* 289: 87–95.
- Huang RQ, Ke W, Han L, Liu Y, Shao K, Jiang C, Pei YY. 2010. Lactoferrin-modified NPs could mediate efficient gene delivery to the brain in vivo. *Brain Res Bull* 81: 600–604.
- Jain RA. 2000. The manufacturing techniques of various drug loaded biodegradable poly(lactide-co-glycolide) devices. *Biomaterials* 21: 2475–2490.
- Joshi DP, Fung YL and Pritchard JW. 1979. Determination of poly (vinyl alcohol) via its complex with boric acid and iodine. *Anal Chim Acta* 104: 153–160.
- Kenneth WY, Mark Miranda GS, Yap Wah Koon T. 1995. Formulation and optimization of two culture media for the production of tumor necrosis factor-b in Escherichia coli. *J Chem Tech Biotechnol* 62: 289-294.
- Konan YN, Gurny R, Allemann E. 2002. Preparation and characterization of sterile and freeze-dried sub-200nm NPs. *Int J Pharm* 233:239-52.
- Labhasetwar V. 1997. Nanoparticles for drug delivery. *Pharm News* 4: 28–31.
- Langer R. 1997. Tissue engineering: a new field and its challenges. *Pharm Res* 14(7): 840–841.
- Levison KK, Takayama K, Isowa K, Okaba K, Nagai T. 1994. Formulation optimization of indomethacin gels containing a combination of three kinds of cyclic monoterpenes as percutaneous penetration enhancers. *J Pharm Sci* 83:1367-1372.
- Michael C, Ilia F, Haim DD, Gershon G. 2002. Lipophilic drug loaded nanospheres prepared by nanoprecipitation: effect of formulation variables on size, drug recovery and release kinetics. *J Control Release* 83: 389–400.
- Minko T. 2004. Drug targeting to the colon with lactins and neoglycoconjugates. *Adv Drug Deliv Rev* 56-491.
- Misra A., Sheth AK. 2002. Mathematical modeling of preparation of acyclovir liposomes:reverse phase evaporation method. *J Pharm Pharmaceut Sci* 5(3): 285-291.
- Moghimi SM, Hedeman H, Muir IS, Illum L, Davis SS. 1993. An investigation of the filtration capacity and the fate of large filtered sterically-stabilized microspheres in rat spleen. *Biochin Biophys ACTA* 1157: 233–240.

- Moghimi SM, Hunter AC and Murray JC. 2001. Long-circulating and target specific NPs: theory to practice. *Pharmacol Rev* 53 (2): 283–318.
- Sahoo SK and Labhasetwar V. 2005. Enhanced Antiproliferative Activity of Transferrin-Conjugated Paclitaxel-Loaded Nanoparticles Is Mediated via Sustained Intracellular Drug Retention. *Mol Pharm* 2(5): 373-383.
- Sahoo SK, Panyam J, Prabha S and Labhasetwar V. 2002. Residual polyvinyl alcohol associated with poly (lactide-co-glycolide) NPs affects their physical properties and cellular uptake. *J Control Rel* 82(1): 105-114.
- Sahoo SK, Wenxue MA and Labhasetwar V. 2004. Efficacy of transferrin-conjugated paclitaxel-loaded Nanoparticles in a murine model of prostate cancer. *Int J Cancer* 112: 335–340.
- Sameti M, Bohr G, Kumar R, Kneuer C, Bakowsky U, Nacken M, Schmidt H, Lehr C, 2003. Stabilisation by freeze-drying of cationically modified silica NPs for gene delivery. *Int J Pharm* 266: 51–60.
- Scholes PD, Coombes AGA, Illum L, Davis SS, Davies MC. 1993. The preparation of sub-200 nm poly (lactide-co-glycolide) microspheres for site-specific drug delivery. *J Control Rel* 25:145–153.
- Sharma A. Sharma S and Khuller GK. 2004. Lectin-functionalized poly (lactide-co-glycolide) NPs as oral/aerosolized antitubercular drug carriers for treatment of tuberculosis. *Journal of Antimicrobial Chemotherapy* 54: 761–766.
- Shirakura O, Yamada M, Hashimoto M, Ishimaru S, Takayama K, Nagai T. 1991. PS design using computer optimization technique. *Drug Dev Ind Pharm*17:471-483.
- Technical Bulletin K0520- solvent miscibility chart and viscosity chart, The HPLC solvent guide, Wiley interscience. 2002.
- www.jtbaker.com/ msds.
- Xiangrong S, Zhao Y, Hou S, Xu F, Zhao R, He J, Cai Z, Li Y, Chen Q. 2008b. Dual agents loaded PLGA NPs: systematic study of PS and drug entrapment efficiency. *Eur J pharm Biopharm* 69 : 445-453.
- Xiangrong S, Zhao Y, Wu W, Bi Y, Cai Z, Chen Q, Li Y, Hou S. 2008a. PLGA NPs simultaneously loaded with vincristine sulfate and verapamil hydrochloride: Systematic study of PS and drug entrapment efficiency. *Int J Pharm* 350 : 320–329.